GEOLOGICAL SURVEY OF CANADA

DEPARTMENT OF ENERGY, MINES AND RESOURCES

PAPER 73-32

# STRATIGRAPHY AND PALEOMAGNETISM OF MOUNT EDZIZA VOLCANIC COMPLEX, NORTHWESTERN BRITISH COLUMBIA

(Report, 17 figures and 3 plates)

J. G. Souther and D. T. A. Symons

CANADA

GEOLOGICAL SURVEY
OF CANADA

PAPER 73-32

# STRATIGRAPHY AND PALEOMAGNETISM OF MOUNT EDZIZA VOLCANIC COMPLEX, NORTHWESTERN BRITISH COLUMBIA

J. G. Souther and D. T. A. Symons

DEPARTMENT OF ENERGY, MINES AND RESOURCES

Available by mail from *Information Canada*, Ottawa

from the Geological Survey of Canada
601 Booth St., Ottawa

and

*Information Canada* bookshops in

HALIFAX — 1683 Barrington Street
MONTREAL — 640 St. Catherine Street W.
OTTAWA — 171 Slater Street
TORONTO — 221 Yonge Street
WINNIPEG — 393 Portage Avenue
VANCOUVER — 800 Granville Street

or through your bookseller

A deposit copy of this publication is also available
for reference in public libraries across Canada

Price: $2.50 Catalogue No. M44-73-32

Price subject to change without notice

*Information Canada*
Ottawa
1974

CONTENTS



## Illustrations

## ABSTRACT

Mount Edziza is the largest and most complex in a group of Late Tertiary and Quaternary volcanoes that lie along a north-south zone of normal faults along the eastern side of the Coast Geanticline in northwestern British Columbia. It is a composite shield and dome in which flat-lying lavas and pyroclastic rocks rest unconformably on tilted lavas and clastic sediments of the Early Tertiary Sloko and Sustut groups.

The products of Mount Edziza belong entirely to the alkali rock series and vary in composition from alkali olivine basalt through trachybasalt to peralkaline trachyte and sodic rhyolite. At least four principal magmatic cycles or stages are recognized. Each stage began with eruption of a primary basalt and culminated with eruption of a more acid phase. Rocks belonging to the earliest stages have been deeply dissected whereas the youngest flows and pyroclastic cones show little or no evidence of erosion.

Detailed paleomagnetic polarity profiles of three stratigraphic sections indicate that six reversals in the earth's magnetic field occurred during the life of the volcano. Correlation of the polarity events with radiometric ages and glacial stratigraphy indicates that volcanic activity began about 6 m.y. B.P., during magnetozone 14, and continued intermittently throughout Pleistocene and into Recent time. During this long interval, successive centres of eruption were confined to a zone within a few miles of the present crater of Mount Edziza. Moreover, there is no evidence of progressive change in the character of the primary alkali olivine basalt, or its peralkaline fractionation products, that issued during the four successive stages of activity.

Thus the volcanicity of Mount Edziza appears to reflect a consistent tectonic environment that has persisted throughout Late Tertiary and Quaternary time. The peralkaline nature of the Edziza lavas and their association with north-south normal faults suggests a zone of crustal rifting.

## RÉSUMÉ

Le mont Edziza est le plus grand et le plus complexe d'un groupe de volcans, datant de la fin de l'ère tertiaire et de l'ère quaternaire, qui s'écnelonnent tout au long d'une zone nord-sud de failles normales s'étendant le long du versant oriental du géanticlinal côtier, dans le nord-ouest de la Colombie-Britannique. C'est un bouclier et un dôme composite, dans lequel de la lave et des roches pyroclastiques disposées en couches planes reposent suivant une discordance angulaire sur de la lave et des sédiments clastiques des groupes Sloko et Sustut, datant du début de l'ère tertiaire.

Les produits du mont Edziza appartiennent entièrement à la série des roches alcalines et leur composition varie du basalte d'olivine alcalin au trachyte peralcalin et à la rhyolite sodique, en passant par le trachybasalte. On reconnaît au moins quatre principaux cycles ou étapes magmatiques. Chaque étape a commencé par l'éruption d'un basalte primaire et a atteint son point culminant avec l'éruption d'une phase plus acide. Les roches appartenant aux étapes les plus anciennes ont été profondément morcelées tandis que les coulées et les cônes pyroclastiques les plus récents ne montrent que peu ou pas d'évidence d'érosion.

Les profils de polarité paléomagnétique détaillés de trois sections stratigraphiques indiquent que six inversions de sens du champ magnétique

de la terre se sont produites au cours de la vie du volcan. La corrélation des résultats se rapportant à la polarité avec les âges radiométriques et la stratigraphie glaciaire indique que l'activité volcanique a commencé il y a six millions d'années B.P., au cours de la magnétozone 14, et s'est poursuivie par intermittence pendant tout le Pléistocène jusqu'au début de l'ère récente. Au cours de ce long intervalle, les centres successifs d'éruption ont été restreints à une zone située dans un rayon de quelques milles de l'actuel cratère du mont Edziza. En outre, il n'existe aucune évidence d'un changement graduel dans la nature du basalte d'olivine alcalin primaire ou dans les produits de fractionnement peralcalins qui ont été émis par le volcan au cours de ses quatre étapes successives d'activité.

Le volcanisme du mont Edziza semble donc indiquer un environnement tectonique constant qui a persisté pendant toute la fin du Tertiaire et au Quaternaire. La nature peralcaline de la lave Edziza et son association avec des failles normales affectant la direction nord-sud fait supposer une zone de fissures de la croûte.

# STRATIGRAPHY AND PALEOMAGNETISM OF MOUNT EDZIZA VOLCANIC COMPLEX, NORTHWESTERN BRITISH COLUMBIA

## INTRODUCTION

Upper Tertiary and Quaternary volcanic rocks are widespread in northwestern British Columbia but few of them have been dated precisely and little is known about the correlation of events between adjacent eruptive centres. Many post-glacial pyroclastic cones have a linear distribution, suggesting that they are spatially related to fundamental fractures. However, the temporal relationships, so important to concepts of regional and global tectonics, have yet to be worked out. Thus it is not known whether eruption of several volcanoes occured more or less simultaneously, in response to


Figure 1. Index map

Original manuscript submitted: 14 August, 1973
Final version approved for publication: 27 November 1973

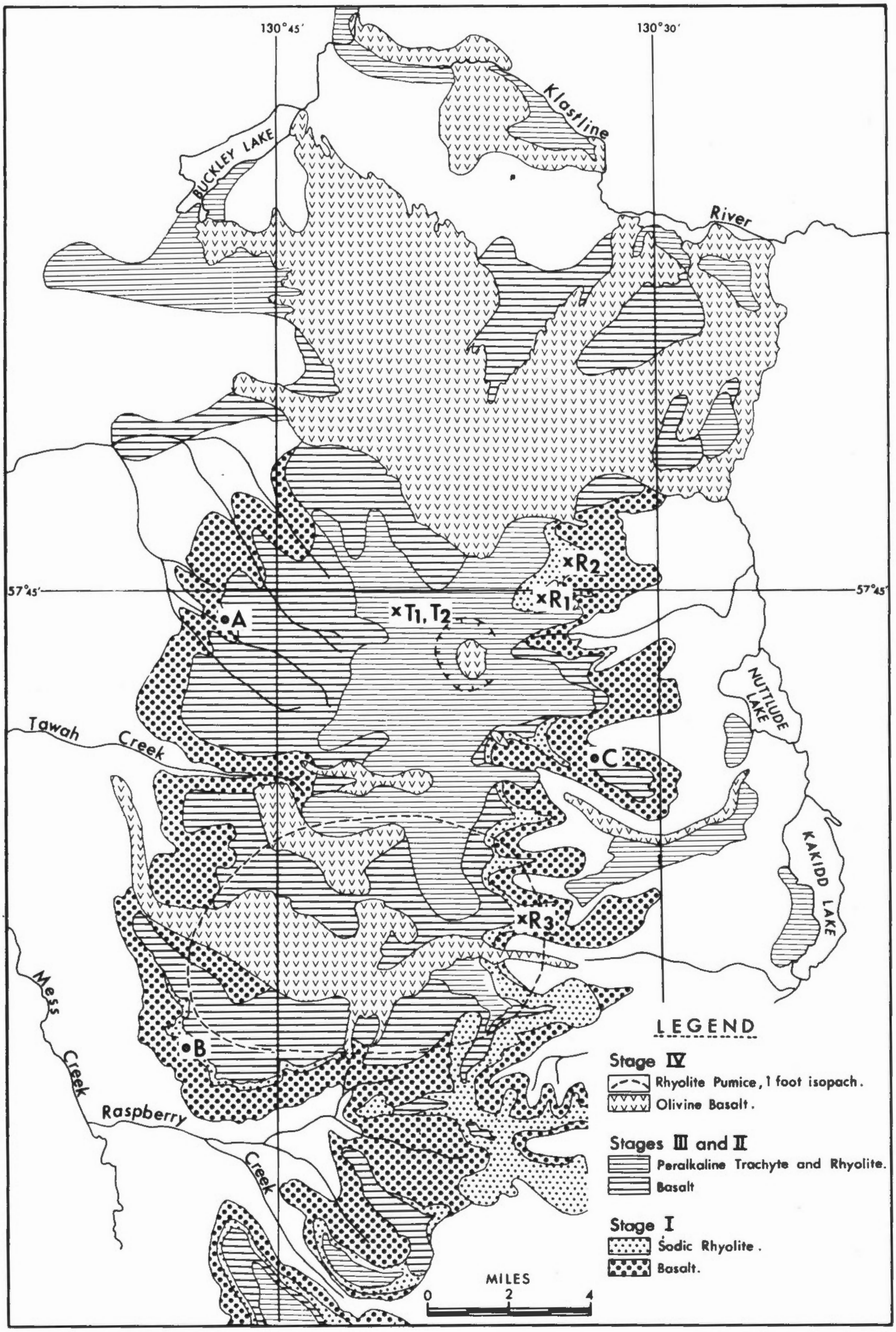


Figure 2. Generalized geological map of Mount Edziza volcanic complex. A, B, and C indicate locations of measured sections. $T_1$, $T_2$, $T_3$ trachyte and $R_1$, $R_2$, $R_3$ rhyolite specimens from central cone.

some specific tectonic event, or whether each centre erupted independently and at random. Nor is it known whether the character of lavas changed systematically with time or whether the varied assemblage within each pile is the result of local and unique conditions of fractionation.

With these problems in mind the present reconnaissance study was undertaken to establish the sequence and age of a typical succession of late Tertiary and Quaternary lavas in northwestern British Columbia. Mount Edziza was selected because there the lavas are flat lying and of varied composition, and because their eruption is known to have spanned an interval of several million years. The stratigraphy, petrography, and paleomagnetic polarity profiles of three sections of Edziza lavas are presented.

## TECTONIC SETTING

Mount Edziza and the adjacent Spectrum Range lie along the eastern margin of the Coast Geanticline, the core of which is a complex of Mesozoic and Lower Tertiary granitic and metamorphic rocks that extends northwesterly for one thousand miles from Washington to Alaska (Fig. 1). During the late Cretaceous and early Tertiary, uplift of the Coast Geanticline was accompanied by emplacement of many high level granitic plutons and eruption of acid to intermediate lavas of the Sloko Group (Souther, 1971). This episode of volcanicity culminated in the Eocene with the explosive eruption of vast sheets of acid pyroclastic material from numerous vents along the eastern flank of the Coast Geanticline (Souther, 1967). Volcanism was accompanied by extensive north-south block faulting and locally by cauldron subsidence (Lambert, 1968). The duration of this episode of volcanicity is unknown. In southern British Columbia a period of quiescence during the Oligocene appears to have separated Kamloops (mid-Eocene) volcanism from the eruption of plateau basalt in the mid-Miocene (Rouse and Mathews, 1961). In northern British Columbia Sloko volcanism may have persisted longer, extending into Oligocene or even early Miocene time. In any case steeply tilted, locally folded Sloko strata were truncated by a fairly mature erosion surface prior to eruption of the first Edziza flows.

Many of the Upper Tertiary and Quaternary volcanoes in northwestern British Columbia including Mount Edziza lie along linear north-south belts parallel with the direction of early Tertiary block faulting and extending obliquely across the regional northwesterly Cordilleran structural trend. During the growth of the volcano, periodic movement on several of these faults resulted in progressively greater offset of the older Edziza lavas (Souther, 1970). Apart from this normal fault movement, the flows of Mount Edziza are undeformed.

## GEOLOGY AND PHYSIOGRAPHY

Mount Edziza volcanic complex (Fig. 2) consists of Mount Edziza volcano, dissected lava domes of the Spectrum Range, and a host of satellitic cones that surround the main vent. The basal part is a basaltic shield about forty miles long and fifteen miles across consisting of thin, flat-lying flows of columnar basalt alternating with beds of loose scoria and pumiceous ash. Superimposed on the northern part of this shield the composite dome of Mount Edziza rises to a circular summit crater about 1 1/2 miles in diameter at an

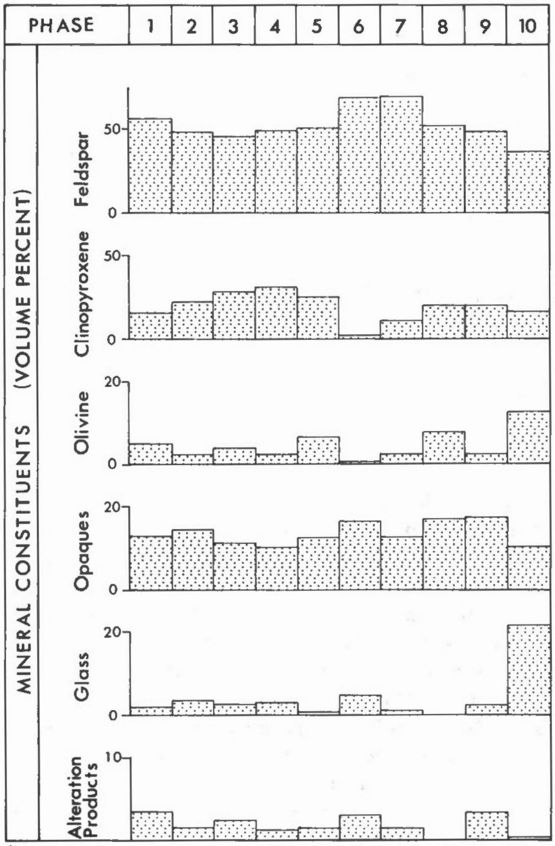


Figure 3. Average modes of basaltic rocks from sections A, B, and C. Includes only rocks with less than 10 per cent alteration products.

elevation of over 9,000 feet above sea level. In contrast to the lower shield the central dome includes lavas and pyroclastic rocks of widely varied composition and mode of eruption. The more basic, and hence more fluid, lavas flowed far out across the surface of the shield whereas the more acid lava piled up near the central vent in thick stubby flows or lava domes. These rocks, mainly of trachytic and rhyolitic composition, are responsible for most of the high relief in the central part of the mountain. Part of the acid magma erupted explosively to form ash flows and ash falls of wide extent.

The evolution of Mount Edziza spans the Pleistocene Epoch and hence the stratigraphy of the volcanic rocks reflects the ebb and flow of continental ice sheets and alpine glaciers. Tills, glacial-fluvial, and glacial-lacustrine deposits are interbedded with the flows. Subglacial eruptions produced piles of hyaloclastite and pillow lava whereas ash and rubble, saturated with glacial meltwater, formed lahars that swept down the slopes of the mountain onto the surface of the shield. Post-glacial activity was confined to satellitic vents that erupted around the base of the main dome and formed cinder cones and extensive fields of blocky, olivine basalt that spread out on the surface of the shield or formed intra-canyon flows in the radial valleys incised into the lower part of the mountain.

## PETROGRAPHY

All of the Edziza lavas belong to the alkaline rock series. They were emplaced during at least four principal cycles (stages) of activity, each beginning with effusion of a relatively large volume of fluid basalt and culminating with eruption of a relatively small volume of more acid magma (Souther, 1971). Within the complex there is a fairly complete spectrum of rocks ranging from picritic alkali olivine basalt through trachybasalt to peralkaline trachyte and sodic rhyolite (comendite). The more acid flows are confined to

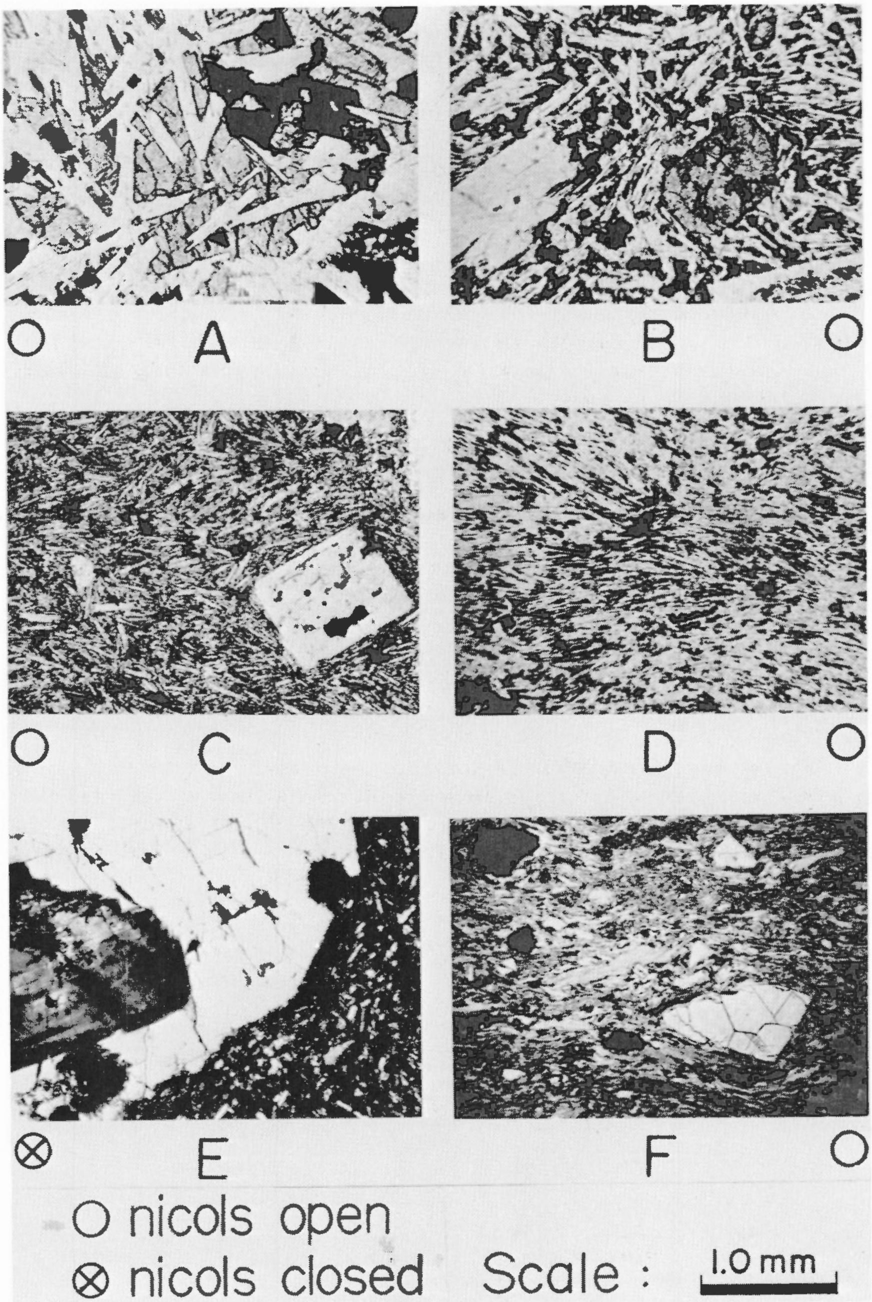


A. Ophitic basalt (unit B3).
B. Intergranular basalt (unit A11).
C. Trachybasalt (unit A26)
D. Trachyte ($T_1$)
E. Porphyritic comendite ($R_2$). Large phenocryst of sodic plagioclase with thick anorthoclase rim.
F. Welded ashflow (unit B27)

Plate I. Photomicrographs.

the central part of the mountain and only the related pyroclastic materials are present in the outer part of the shield where the three stratigraphic sections were measured. Petrographic and chemical data on these lavas are from specimens of trachyte ($T_1$, $T_2$) and rhyolite ($R_1$, $R_2$, $R_3$) collected near the summit of Mount Edziza (Fig. 2). All other data are from samples collected from the three measured sections. These are tabulated in Appendix II and summarized in Figures 3 and 4. Volumetric analyses, made with an automatic traversing stage, are based on a minimum of 1,000 points for fine-grained uniform rocks and 3,000 points for porphyritic rocks. Mineral compositions are estimated from their optical properties.

A brief description of the principal rock types is given below. Each of these includes varieties with distinctive textural or mineralogical features, described in the later section on stratigraphy, that can be used as a basis for local correlation.

## Basalt

Two types of alkali olivine basalt can be distinguished on the basis of texture and composition of the clinopyroxene. The first (Pl. Ia) is characterized by large, ophitic to subophitic plates of deep purple titanaugite (2V 55°) which enclose randomly oriented plagioclase laths, euhedral crystals of olivine, and magnetite grains. The second (Pl. Ib) has a characteristic intergranular texture in which clear or pale green subhedral crystals of sodic augite (2V 75°) and magnetite form a granular mosaic between the feldspar laths. The latter are commonly oriented and may give the rock a trachytic texture.

Sparse phenocrysts of plagioclase are present in both types of basalt and in a few flows they form up to 40 per cent of the rock. They are thin, tabular, up to 3 cm long, and commonly display both polysynthetic and Carlsbad twinning. The cores are labradorite but the type and extent of

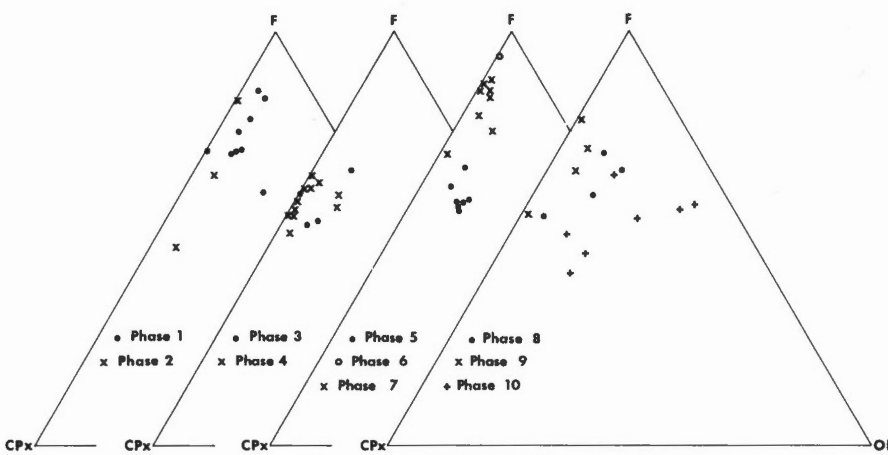


Figure 4. Triangular plots of modal feldspar (F), clinopyroxene (CPx), and olivine (Ol) for basaltic rocks erupted during the ten phases of Edziza activity. Includes only rocks with less than 10 per cent alteration products.

zoning varies even within a single thin section. Many crystals are unzoned except for a narrow rim in which the composition changes to that of the groundmass feldspar. Others exhibit normal or complex oscillatory zoning throughout most of the crystal. In nearly all cases the outermost rim is reversely zoned.

Groundmass feldspar forms ragged, subhedral laths that are commonly zoned from about $An_{60}$ to $An_{40}$.

Olivine as microphenocrysts and tiny intergranular euhedra in the groundmass rarely comprises more than 5 per cent of the rock. The crystal boundaries are sharp and are not surrounded by reaction rims. Iddingsite in uncommon.

The groundmass and phenocrystic plagioclase crystals are surrounded by potash plagioclase (potash andesine) in optical continuity and minute amounts of alkali feldspar (calcic anorthoclase) fill small interstices.

The groundmass of the basalts generally includes a small amount of brown glass and/or pale green or yellow chlorophaeite. Vapour phase crystals of calcite, aragonite, hydrous iron oxides and rarely brown hornblende are sporadically distributed.

## Trachybasalt

The trachybasalts grade on the one hand into alkali olivine basalts, from which they differ in the more sodic nature of their average feldspar, and on the other into trachytes. The texture is invariably trachytic (Pl. Ic). Oriented laths of plagioclase form 60 to 80 per cent of the rock and enclose an intergranular matrix of augite crystals, granular magnetite, and anhedral alkali feldspar. The groundmass plagioclase is zoned from about $An_{50}$ to about $An_{30}$ and is surrounded by irregular rims of potash plagioclase in optical continuity. Augite phenocrysts are commonly surrounded by overgrowths of pale green aegirine-augite.

## Trachyte

The trachytes (Pl. Id) differ from the trachybasalts in their higher content of alkali feldspar and much lower content of mafic minerals. Very thin tabular phenocrysts of clear sanidine and/or sodic plagioclase from 2 to 3 millimetres long are enclosed in a deuterically altered pilotaxitic matrix of feldspar microlites, glass, and very fine magnetite granules. Most sections contain aegirine, and aegirine-augite either as groundmass minerals or as small phenocrysts from 1 to 2 millimetres long. In addition many of the trachytes contain irregular clusters of arfvedsonite and aenigmatite crystals in the groundmass (Yagi and Souther, in prep.).

## Sodic Rhyolite (Comendite)

Many of the rhyolites are completely glassy or contain only tiny crystallites of feldspar, aegirine, and the bright red alkalic amphibole, aenigmatite. Fine-grained crystalline varieties contain clear, euhedral phenocrysts of strongly zoned sodic plagioclase with thick mantles of anorthoclase in optical continuity (Pl. Ie).

Devitrified and deuterically altered rhyolite is common. It usually displays spherulitic or orbicular textures and invariably contains abundant tridymite.

Figure 5. Chemical compositions of Mount Edziza Lavas.

| | 1 | 2 | 3 | 4 | 5 | 6 | 7 | 8 | 9 |
|---|---|---|---|---|---|---|---|---|---|
| $SiO_2$ | 47.6 | 75.8 | 64.3 | 55.3 | 59.2 | 66.1 | 47.8 | 51.3 | 51.2 |
| $Al_2O_3$ | 17.5 | 12.7 | 19.4 | 18.1 | 19.3 | 13.7 | 13.8 | 21.0 | 18.5 |
| $Fe_2O_3$ | 12.3 | 3.0 | 2.5 | 8.3 | 6.1 | 8.6 | 14.1 | 8.1 | 10.3 |
| MgO | 4.8 | 0.5 | 1.2 | 1.9 | 1.1 | 0.7 | 16.0 | 3.5 | 4.4 |
| CaO | 9.3 | 0.3 | 1.8 | 5.1 | 1.0 | 1.2 | 6.7 | 9.5 | 8.8 |
| $Na_2O$ | 3.4 | 5.0 | 5.3 | 5.3 | 6.9 | 5.7 | 3.0 | 4.3 | 4.3 |
| $K_2O$ | 1.1 | 3.9 | 5.1 | 3.5 | 5.1 | 4.5 | 0.90 | 1.4 | 1.5 |
| $TiO_2$ | 2.32 | 0.18 | 0.25 | 1.24 | 0.20 | 0.46 | 1.44 | 1.43 | 1.74 |
| MnO | 0.18 | 0.04 | 0.06 | 0.22 | 0.17 | 0.22 | 0.19 | 0.11 | 0.16 |

1. Phase 4 basalt from unit A3 (No. 916)*
2. Stage I sodic rhyolite (R1) from central cone (No. 924)
3. Stage I sodic rhyolite (R2) from central cone (No. 925)
4. Phase 7 trachybasalt from unit C20 (No. 919)
5. Stage III trachyte (T1) from central cone (No. 922)
6. Stage III trachyte (T2) from central cone (No. 917)
7. Phase 9 basalt from unit A24 (No. 920)
8. Phase 10 basalt from unit A27 (No. 921)
9. Phase 10 basalt from unit A28 (No. 918)

* Geological Survey of Canada, laboratory number.

## CHEMISTRY

Discussion of the petrochemistry of the Edziza lavas is beyond the scope of this paper. The nine chemical analyses listed in Figure 5 show the range of chemical variation within the Edziza pile and support the petrographic evidence for its alkaline affinity. A plot of total alkalis versus silica (Fig. 6) indicates that the analyzed rocks fall well within the field of the alkali rock series (Kuno, 1968) and that they differ markedly from the calc alkaline trends of Mount Garibaldi (Mathews, 1958) and the high Cascades farther south (Kuno, 1969).

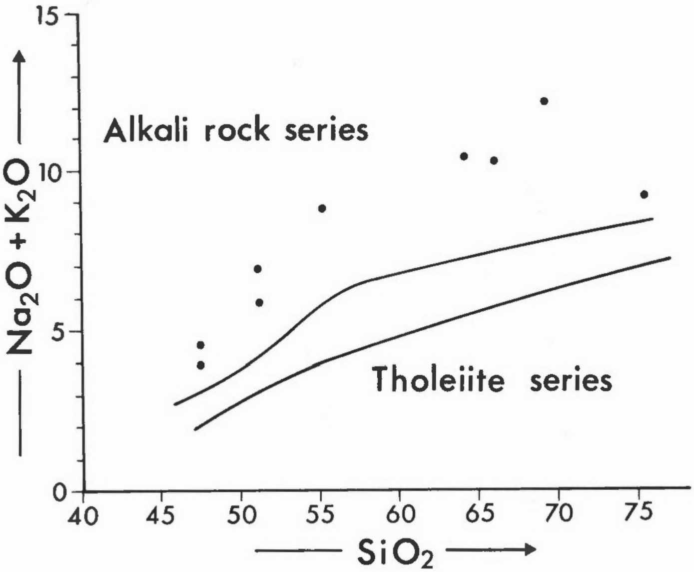


Figure 6
Alkali-silica diagram for Edziza lavas. Boundary lines are from Kuno (1968).

| Generalized succession | | Phases present in stratigraphic sections A, B, and C |
|---|---|---|
| Stage | Lithology | |
| IV | Rhyolite pumice | |
| | Basalt from satellitic vents | 10 |
| III | Trachyte and trachybasalt of the central cone of Mount Edziza | |
| | Basalt of upper shield | 7, 8, 9 |
| II | Rhyolite and trachyte flows, domes and pyroclastic rocks | |
| | Trachybasalt flows | 6 |
| | Basalt of middle shield | 3, 4, 5 |
| I | Rhyolite and trachyte lava and ash flows | 2 |
| | Basalt of lower shield | 1 |

Figure 7. Correlation chart showing relationship of the ten phases sampled in stratigraphic sections A, B, and C to the generalized succession for the Edziza complex as a whole.

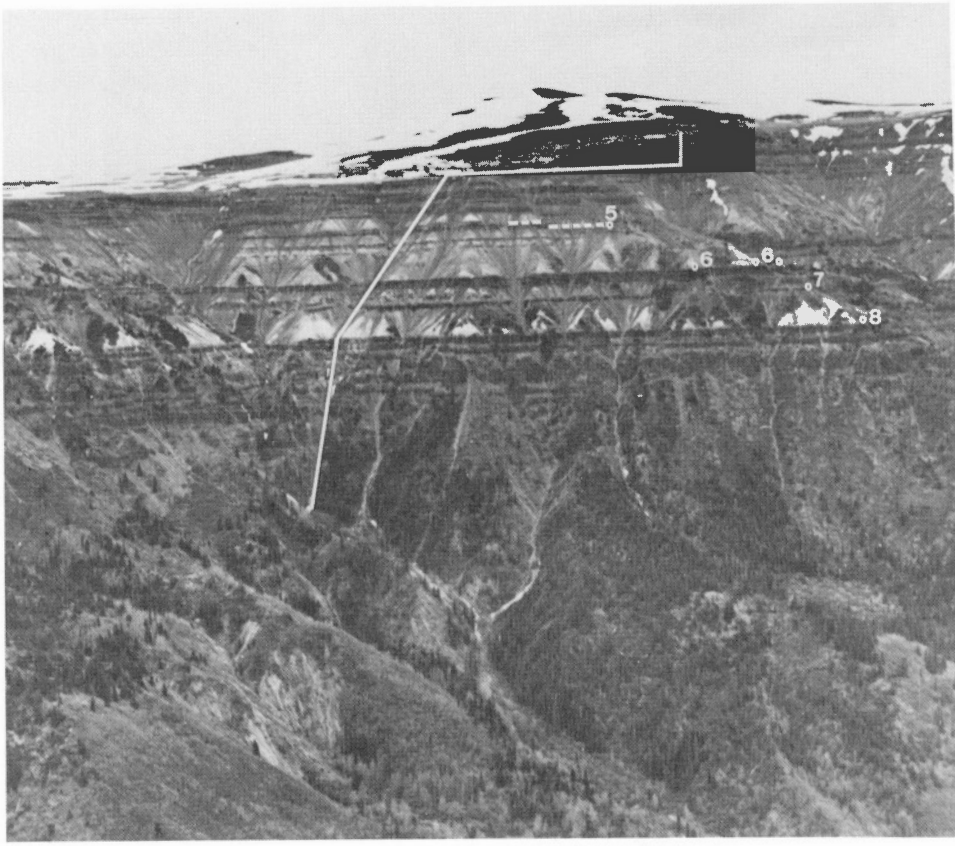


Plate II. Photograph of escarpment on the west side of Mount Edziza, showing location of section B. Low conical hill on plateau surface is a pile of phase $10_1$ sideromelane tuff-breccia and pillow lava.

## STRATIGRAPHY

Radial valleys cut into the flanks of Mount Edziza expose stratigraphic sections of both the central dome and the basal shield part of the volcano (Pl. II). Facies changes from the vent outward are very rapid. Thick lava flows and domes in the central part of the complex are represented by thin ash layers on the flanks and conversely, thick glacial and fluvial deposits on the flanks of the mountain may be completely absent in the steeper central part. In selecting sections for study (Fig. 2) an attempt was made to compromise between these two extremes in order to get as complete a record of volcanism as possible and yet include the major glacial and fluvial layers which record natural breaks in the sequence of volcanic eruptions.

The history of Mount Edziza may be divided into at least four principal magmatic cycles or "stages" (Fig. 7). Each "stage" comprises several discrete "phases" of eruption from one or more vents. The products of a given "phase" comprise an "assemblage" of closely related cooling units. In this paper the term "phase" is used in a time-stratigraphic sense to denote

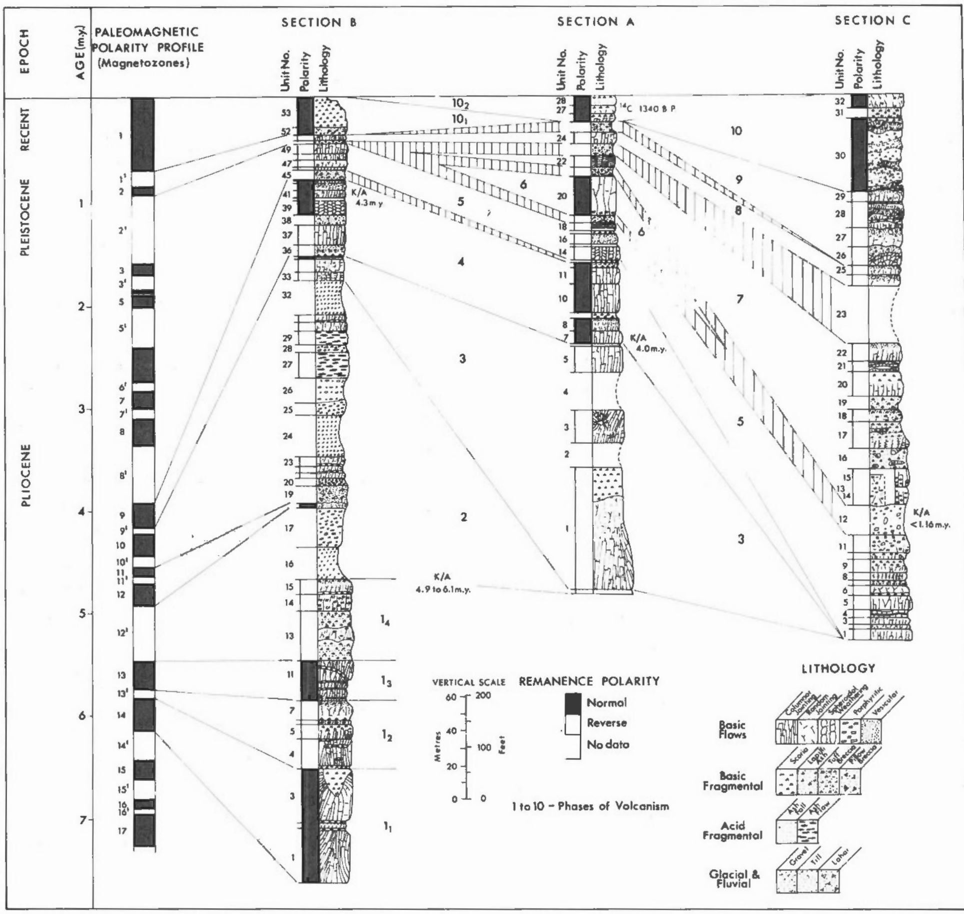


Figure 8. Correlation chart showing stratigraphic columns, lithology and magnetic polarity profiles of three sections (A, B, and C) of Edziza lavas.

all the products deposited during a given interval of time. Consecutive phases are numbered from oldest to youngest and dissimilar lava assemblages erupted during the same phase are designated as sub-phases, $1_1$, $1_2$, etc. Individual units are numbered consecutively from oldest to youngest in each stratigrahpic section and designated by section letter and unit number, A1, A2, etc.

Details of the three measured sections are presented in Appendix I and shown diagrammatically in Figure 8. Thicknesses were measured directly with a tape and elevations determined by a sensitive, surveying altimeter corrected for diurnal change against a continuous recording barograph.

## Phase 1

The lavas of phase 1 which comprise the basal shield of Mount Edziza, and Spectrum Range are an apparently uniform succession of rusty to dark reddish brown weathering columnar flows separated by thick mats of loose, highly oxidized scoria. The fresh rock is medium grained to fine grained dark bluish grey basalt with a variable content of plagioclase and rarely pyroxene phenocrysts. The flows of the basal shield exhibit a systematic upward increase in the content of plagioclase phenocrysts. In section B this trend is repeated three times, culminating in flows B6, B10, and B14. The latter contains from 40 to 50 per cent plagioclase phenocrysts up to 3 centimetres across and forms a persistent horizon marker along the entire western part of the complex.

Except for the variation in phenocrystic plagioclase the phase 1 flows are remarkably uniform in their mineralogy and texture. Randomly oriented or crudely aligned euhedral to subhedral laths of labradorite, sparse euhedral to rounded crystals of olivine and granular magnetite are enclosed by clinopyroxene which, with the exceptions noted below, has the deep purple colour of titaniferous augite. Alkali feldspar, which may form up to 10 per cent of the total feldspar, is interstitial to all other minerals. Accessories are apatite, which is ubiquitous, and very small amounts of pale red spinel. A few flows exhibit minor variations. The basal flow of section B is anomalously rich in olivine. This is probably due to crystal settling since only the base of this very thick, cliff-forming unit could be reached for sampling. In flows B7 to B12 inclusive, the pyroxene is not as deeply pigmented as the purple titaniferous augite that characterizes the remainder of the assemblage. Moreover this relatively clear pyroxene tends to occur as small subhedral intergranular crystals rather than as ophitic plates. This difference may be due to differences in the cooling history rather than to differences in original composition. Flows containing the clear pyroxene also contain a high proportion of interstitial glass which is commonly charged with microlites of pyroxene and ilmenite and may have a bulk composition close to that of titanaugite.

The phase 1 rocks are free from weathering products but most have undergone at least some deuteric alteration. This is most apparent in the lower flows in which parts of the interstitial glass and pyroxene have been selectively replaced by carbonate, hydrous iron oxides, and chlorophaeite. Alteration is patchy, being most intense around vesicles from which late magmatic fluids have diffused outward into the surrounding rock. Many of the vesicles have been partly or completely filled with radiating clusters of aragonite, or lined with botryoidal encrustations of goethite.

## Phase 2

This very complex assemblage is characterized by the alternation of basaltic lava flows with rhyolitic ash falls and ash flows. It is best preserved in section B which contains, in addition to the primary volcanic products, thick fluvial and glacial-fluvial deposits. The ash flows thin rapidly northward and, at section A, only a thin layer of fine white phase 2 ash separates the lowest basalt from pre-Edziza basement rocks.

In section B the lower two pumice falls, B16 and B24, comprise white, unconsolidated pumiceous ash in which highly vesiculated fragments are well sorted and mostly less than 2 millimetres in diameter. Many exhibit elongate, spindle-shapes with very fine linear vesiculation. In addition to pumice the ash contains from 10 to 25 per cent crystal fragments including sanidine, quartz, sodic plagioclase and a trace of aegirine.

Units B27 and B29, near the centre of the phase 2 pile, are highly welded ash flows (Pl. If) separated by a thin layer of fluvial gravel. Both are prominent, orange-weathering, cliff-forming members with widely spaced, vertical jointing. Slight variations in the degree of welding suggest that the lower, thicker flow may be a composite of two cooling units. The base of both ash flows is a densely welded, black, vitreous layer with prominent taxitic texture. This rests on a thin layer of air-fall pumice and grades upward into the moderately welded central part of the flow. The ash flows are characterized throughout by the presence of numerous lithic and crystal fragments, and by greatly attenuated lenticles of black, glassy obsidian. The latter vary from a few centimetres to more than 50 centimetres in length and from a few millimetres to 10 centimetres in thickness. Lithic fragments, from microscopic grains up to blocks 20 centimetres across, consist of cognate rhyolite fragments and accidental clasts of fine-grained basalt.

Thin sections reveal that the bulk of the flows consist of small vitreous shards which, near the base, have been completely flattened and smeared out into flow layers. Throughout the remainder of the flow they are moderately compressed and welded, displaying a prominent taxitic banding that wraps around lithic and crystal fragments as well as the larger fragments of porous, partly collapsed pumice. Crystalline material consists mainly of broken and euhedral crystals of sanidine, quartz, and sodic plagioclase. A few thin sections contain tiny crystals of aegirine. The vitreous black lenticles are clear, structureless glass with sparse sanidine microlites and tiny needles of aegirine.

The uppermost phase 2 ash fall (B32) is fine, white, unconsolidated pumiceous ash, similar to the lower two ash falls (B16 and B25), but with a much higher content of crystals. These include 1- to 2-millimetre euhedral prisms of the dark red sodic amphibole, aenigmatite, in addition to clear laths of sanidine, quartz, plagioclase, and a small amount of aegirine.

The acidic, pyroclastic products of phase 2, alternate with relatively thin, but laterally extensive, basaltic flows (B18, B21, B22, B23, B30, B31). These are very hard, dense, fine-grained flows with surfaces deeply stained by manganese and iron oxides. Their texture is distinctly trachytic. Oriented microlites of plagioclase and sparse microphenocrysts of olivine and titanaugite are surrounded by a granular mosaic of clear, pale green sodic augite and magnetite.

Numerous fluvial deposits preserved between the flows indicate that eruptions during phase 2 were sporadic, and separated by long periods of quiescence. The thick gravel layer (unit B17) that lies above the lower ash fall, consists almost entirely of cobbles and pebbles of white, porphyritic sanidine rhyolite, almost certainly derived from a dome or flow that accompanied eruption of the underlying ash. Thus a long period of erosion must have intervened between the initial eruption of unit 16 and the next pulse of volcanic activity. Moreover the transport of well-rounded and sorted cobbles from the high central part of the mountain to their present position on its flanks indicates that the region was not covered by extensive glaciers at that time.

Subsequent eruption of unit B18 was accompanied by mud slides or lahars (unit B19) suggesting that excessive meltwater from summit glaciers may have been generated by the eruption.

## Phase 3

Phase 3 flows overlie the sodic trachybasalts and rhyolites of phase 2. They are similar texturally and mineralogically to the lower basalts of phase 1 and are considered to be the primary lavas in a new cycle of activity (stage II). Like the early basalts of stage I their texture is ophitic to subophitic with randomly oriented laths of plagioclase and small granules of olivine surrounded by deep purple titanaugite.

## Phase 4

Phase 4 flows are present in sections A and B but were not recognized in section C. They differ from the lavas of phase 3 in both their texture and mineralogy. The pyroxene is clear, pale green augite that occurs with magnetite as subhedral to euhedral grains between the feldspar laths. Microphenocrysts of olivine and strongly zoned titaniferous augite with pronounced hour-glass structure, are present in all thin sections and aegirine-augite occurs as a minor constituent in the uppermost flows. The progressive change in the character of the pyroxene from titanaugite to aegirine-augite suggests that phase 3 and 4 basalts are closely related and that both may be products of a single magma series that fractionated to produce increasingly alkaline lavas.

## Phase 5

In sections A and B, phase 5 lavas are underlain by layers of glacial till (A13-B45) and overlain by fluvial sand and gravel (A19-B50). In section C the lower contact is covered by a thick layer of glacial till and glacial-fluvial gravel overlies the uppermost phase 5 flow. Both units C12 and B45 contain boulders that are not indigenous to the volcano and must have been transported for many miles by glacier ice. Moreover, the gravels associated with the till of unit C12 contain numerous obsidian pebbles that can be traced to their source in nearby rhyolite flows. The latter have yielded K-Ar and fission track ages of 1.16 and 0.9 m.y. respectively. Thus both the age dates and the evidence of glaciation support a Pleistocene age.

The phase 5 flows are characteristically thin and highly vesicular. Joints are closely spaced, either random or crudely columnar and the surface is deeply stained with iron and manganese oxides. The fresh rock is pale grey basalt with tiny flecks of pale yellow limonite. Most thin sections show the texture to be diktytaxitic. Euhedral laths of plagioclase surround and project into numerous microscopic voids which are lined with a very thin film of hydrous iron oxide. Highly titaniferous augite forms ophitic to subophitic plates that enclose both plagioclase and magnetite.

## Phase 6

Only one phase 6 flow (A20) is present in the measured sections, however, it represents an important episode of activity during which numerous thick flows of trachybasalt, trachyte, and several large domes of sodic rhyolite were extruded in the central part of the complex. Unit A20 is more basic than most of the lavas erupted during this phase and, as a result, it had sufficient mobility to flow across the surface of the shield as far west as section A. It is a highly porphyritic alkaline basalt containing more than 20 per cent large plagioclase phenocrysts up to 4 cm long. These are commonly unzoned sodic labradorite except for a thin outer rim that changes to potash andesine. Sparse phenocrysts of iddingsite are pseudomorphous after olivine. The groundmass comprises oriented laths of sodic plagioclase, ragged clusters of pale green sodic pyroxene and granules of magnetite.

The more typical trachybasalts, trachytes and rhyolites of phase 6, were relatively viscous and did not spread far enough from their source to reach the positions of the measured sections. Specimens $R_1$ and $R_2$ (Appendix II, pt. 2), from the central cone of Edziza, are typical of the phase 6 rhyolite. Phenocrysts of sanidine, sodic plagioclase and aegirine-augite are enclosed in a fine-grained matrix of plagioclase, quartz, aegirine, arfvedsonite, aenigmatite and titaniferous magnetite.

## Phase 7

The products of phase 7 occur in section C as irregular flows of basalt and trachybasalt associated with a high proportion of clinker and coarse tephra. They rest on a thick layer of glacial till and glacial-fluvial material (C12) and are overlain by a thick, partly covered recessive unit that appears to be mainly fine basaltic ash and cinders. The rock is characteristically porphyritic, with plagioclase and augite phenocrysts surrounded by ragged laths of plagioclase in a dark mesostasis highly charged with magnetite granules. Plagioclase phenocrysts are most abundant (up to 35 per cent) in the lowermost flows (C13, C14, and C15). Phenocrysts in these lower flows are unzoned or moderately zoned, however, the complexity and range of zoning in both the groundmass and phenocrystic feldspar increases upward and, in the uppermost flows (C20, C21, and C22) all of the plagioclase crystals have complex oscillatory zoning over a total range of $An_{60}$ to $An_{30}$. Between these two extremes, in units C16 to C19, the phenocrysts are deeply embayed and exhibit complex penetrative replacement by more sodic plagioclase. Pale brown augite occurs throughout as small (1 to 2 millimetres) euhedra.

In section A, a single flow (A22) occupies approximately the same stratigraphic position as units C13 to C22. It is a pale green trachybasalt with prominent platy flow cleavage along which the rock breaks to a lustrous surface resembling phyllite. If it is part of the same episode of volcanicity then it must be a late, more alkaline phase, that issued from a different vent than units C13 to C22.

## Phase 8

Flows assigned to this phase are widely distributed throughout the Mount Edziza complex but nowhere do they form thick or extensive piles. They probably issued from several separate vents all of which were active during the same polarity epoch. The rock is a characteristic pale grey-weathering basalt with a high content of magnetite in the matrix and a relatively high content of titanaugite and olivine phenocrysts. Many of the flows have a picritic layer at the base and a few contain olivine nodules.

## Phase 9

Phase 9 flows were found only in section C. The lower flow, C26, has the glassy texture and closely spaced three dimensional polygonal jointing characteristic of a quenched, subaqueous flow. The upper members, C27 to C29, are very irregular basalt flows associated with coarse tephra including large bombs and spatter which suggest a nearby source. The texture is distinctive. Randomly oriented laths of labradorite are surrounded by a glassy mesostasis containing tiny clear green pyroxene euhedra and grains of magnetite.

### Phase 10

Phase 10 lavas issued from a large number of satellitic vents around the periphery of the main cone of Mount Edziza. The earliest activity (subphase $10_1$) was contemporaneous with a period of extensive alpine glaciation and many of the products are characteristic of subglacial eruptions. The thin, irregular, glassy flow tongues and thick piles of sideromelane tuff-breccia of unit C30 and the pillow breccia and crudely stratified sideromelane tuff-breccia of B52 and B53 are obvious products of subaqueous eruption. The rock is very fine grained to glassy basalt containing fairly abundant phenocrysts of plagioclase and a few of olivine and pyroxene. In addition all members of this sequence contain a few 1- to 10-centimetre fragments or lenticles of partly fused, medium-grained rock resembling granodiorite. Units C31 and C32 are products of sub-aerial eruption but are included with phase 10 because they contain such granitic clasts. It is probable that these two units were deposited on a local pile that emerged above the ice level.

Phase 10 activity postdates the more recent advance of alpine glaciers. The clinkery flow surfaces, cinder cones, and ash beds have been little altered by erosion (Pl. III). They comprise black, highly vesicular, moderately porphyritic basalt with small phenocrysts of plagioclase, pyroxene and olivine. Samples A27 and A28, from closely related cooling units near the south end of Buckley Lake, are typical of the group. Complexly twinned and strongly zoned plagioclase, euhedral crystals of titanaugite and olivine form phenocrysts in a very fine grained matrix of the same minerals plus abundant magnetite granules.

## RADIOMETRIC DATING

At the time of writing only a few of several planned radiometric age determinations had been completed by the Geological Survey of Canada isotope laboratories.

Five preliminary whole rock K/Ar determinations on basalts and rhyolites of stages 1 and 2 give ages ranging from 4.9 to 6.1 m.y. Three K/Ar rock dates on a single sample of phase 5 basalt give values of $3.0 \pm 0.8$ m.y., $4.6 \pm 1.4$ m.y., and $4.1 \pm 1.1$ m.y., with the latter considered to be the most accurate, giving a mean value of $4.0 \pm 0.6$ m.y. Two K/Ar whole rock dates on a single sample of obsidian from a flow correlative with clasts in unit $C_{12}$ give values of $1.14 \pm 0.14$ m.y. and $1.19 \pm 0.13$ m.y. with the former considered to be more accurate, giving a mean value of $1.16 \pm 0.06$ m.y. (R.W. Wanless, pers. comm., 1968).

A radiocarbon age of $1340 \pm 130$ years before present was obtained on charred twigs from a tundra preserved beneath coarse tephra related to unit A27 (Lowdon et al., 1967).

Fission track ages on several samples of Edziza glass have been determined by F. Aumento (pers. comm.). One of these, an obsidian equivalent to clasts in C12 unit, gives an age of 0.96 to 0.96 m.y. and thus agrees well with the K/Ar age on the same material.

Plate III. Eve Cone and blocky, phase $10_2$ lava flows on the northwestern flank of Mount Edziza. Buckley Lake in background. GSC photo 202468.

## PALEOMAGNETISM

Reversals in the earth's magnetic field polarity have been recorded and dated for the past 10 m.y. with considerable accuracy, using a combination of terrestrial lava flows, sea floor sediments, and oceanic magnetic profiles (Cox and Dalrymple, 1967; Heirtzler et al., 1968; Cox, 1969). Thus the magnetic polarity profile of a lava sequence such as Mount Edziza can be useful in correlation and dating especially when used in conjunction with a few radiometric ages. The geomagnetic polarity profile and numbering system for the magnetozones used as the standard for this study (Fig. 7) is taken from Cox (1968).

Paleomagnetic polarity profiles were determined for each of the three measured sections of Edziza lavas, Appendix III. These are plotted with the stratigraphic data in Figure 8 and stereographic plots of individual unit mean remanence vectors are shown in Figure 9.

## Sampling and Laboratory Procedure

Four or more individually oriented cores were collected from each of 91 flow units, using a portable diamond drill. The cores were oriented to within about 2° of arc by a sun compass and/or by topographic triangulation using a Brunton compass and adjacent mountain peaks. With a few exceptions, two cylindrical specimens were cut with dimensions of 1 1/4" diameter and 1 3/16" height from each core. A total of 405 cores yielding 756 specimens were collected.

The natural remanent magnetization (NRM) of each specimen was measured using an automated biastatic magnetometer which is accurate to within 1.0° of arc for a remanence intensity of $1 \times 10^{-6}$ emu/cc or greater (Larochelle and Christie, 1967). One specimen of average NRM direction and intensity from each unit was demagnetized stepwise in peak alternating field (AF) intensities of 25, 50, 75, 100, 200, 300, 400 and 800 oersteds using an AF demagnetization equipment described by Larochelle and Black (1965). For these specimens, the successive change in remanence direction and intensity after each demagnetization step was plotted, and the stability index (Tarling and Symons, 1967) was calculated. Depending on the plots and indices, the rest of the specimens were demagnetized at 200 or 300 oersteds.

## Data Selection

In order to assure reliable mean site or polarity zone remanence directions, unreliable data was filtered out and rejected. To this end, the following sequence of tests were applied:

A) A core was rejected if its NRM proved too weak in intensity ($\leqslant 5 \times 10^{-7}$ emu/cc) in relation to the magnetometer noise level to be reliably measured within 2° of arc.

B) A core was rejected if its remanence after AF demagnetization proved too weak to be measured reliably ($\leqslant 5 \times 10^{-7}$ emu/cc).

C) A core was rejected as unreliable because of possible remanence instability or inhomogeneity if the angle $\theta$ between the remanence directions of its two specimens exceeded 23° which corresponds to a minimum with core precision estimate k (Fisher, 1953) of 25 or greater.

D) A core represented by a single specimen was rejected as unreliable if its remanence direction deviated by more than the angular standard deviation (A.S.D.) (Larochelle, 1968) of the remaining cores from the unit, or if the stability index SI for the unit fell below the lower limit for the stable range of 2.5.

E) A core was rejected if it had an abnormally intense remanence ($> 1 \times 10^{-2}$ emu/cc) which could be indicative of a lightning-induced remanence component.

F) A core - and therefore the unit - was rejected if it was the sole remaining reliable core from the unit.

Using the mean remanence direction for each core and giving each acceptable core unit weight, the unit mean remanence direction was calculated along with its precision estimate and the radius of its cone of 95% confidence $\alpha_{95}$ (Larochelle, 1968).

G) If the values of $\alpha_{95}$ exceeded 10° for a unit with 3 or more cores, then one core was rejected if the divergence of its remanence direction from the mean direction of the remaining cores exceeded three times the A. S. D. from the mean direction; the unit mean statistics were then recalculated.

H) If the value of k falls below 12 for a unit, then the unit was considered metastably or inhomogeneously magnetized.

A detailed listing of rejected cores and of the acceptable remanence data is given in Appendix III.

In practice, criteria A, B, E, and F did not lead to the rejection of any cores. Criterion C led to the rejection of 27 cores including all 12 from 3 units. Criterion D led to the rejection of 20 single-specimen cores which are, nevertheless, grouped in remanence direction about the overall mean direction for the Edziza flows. Criterion G led to the rejection of a further 18 cores whose remanence directions are randomly scattered about the overall mean direction. Thus 16 per cent of the cores are considered to give unreliable measures of the true remanence direction. While the criteria are probably too severe, the remanence direction and polarity determined for any surviving unit becomes highly reliable. The polarity of units failing to meet these 3 rejection requirements is obvious in every case, so all polarity determinations have been included in Figure 8.

Giving each of the 84 valid unit mean remanence directions unit weight, the mean remanence direction for units with normal polarity is as expected nearly antiparallel to those with reversed polarity (Appendix III, pt. 2). After rotating the reversed remanence directions to normal polarity, the overall Mount Edziza volcanic complex mean remanence direction gives a pole position nearly coincident with the present geographic pole. This result agrees with the known position for the Upper Tertiary paleomagnetic field (Wilson, 1971) and with the expected result for a time-average pole position for the past 6 m.y. (Fig. 10).

## CORRELATION

The available geochronological data for the Mount Edziza volcanic complex are summarized in Figure 8, along with the interpreted correlation. In Figure 9 the remanence direction of each unit is shown schematically within this same correlation framework. It is apparent that there is good correspondence between the paleomagnetic events and the stratigraphic subdivisions based on geology and petrography. It is also apparent that the

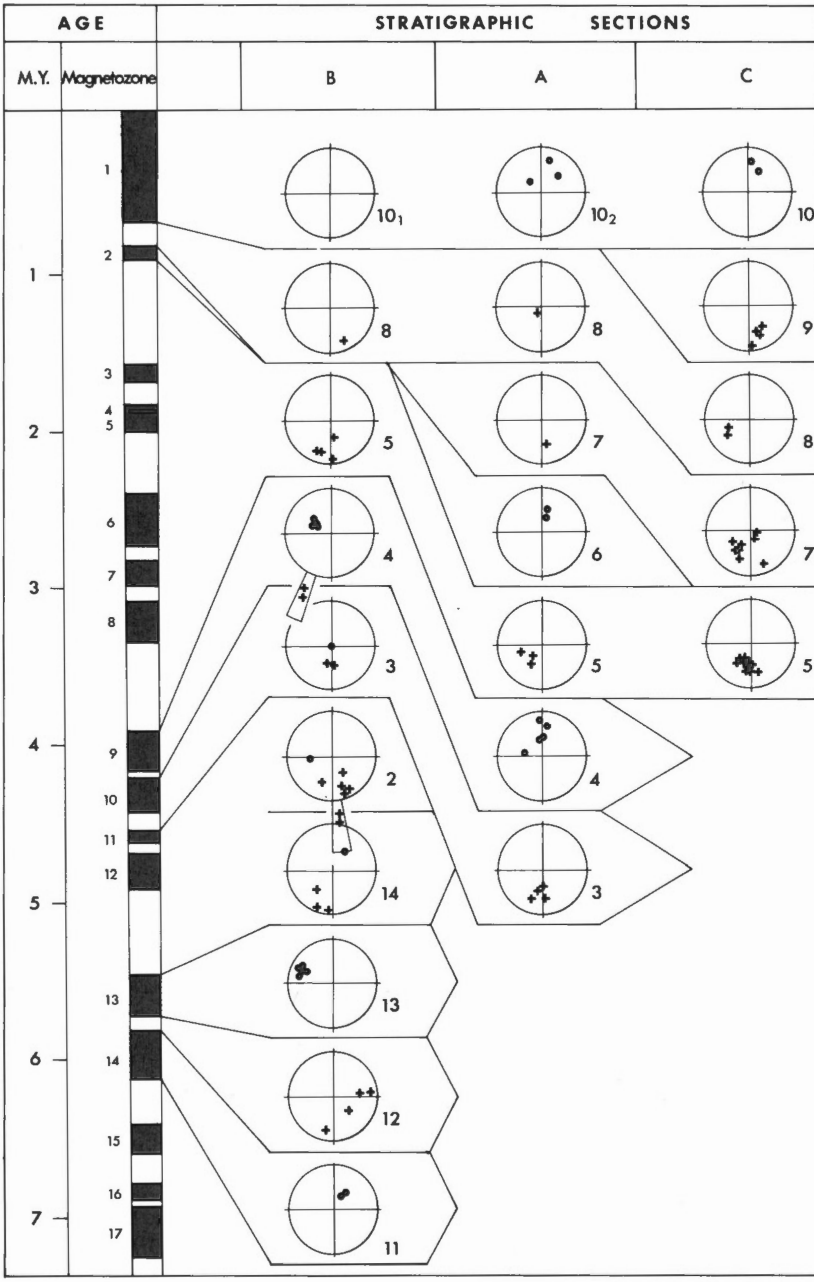


Figure 9. Correlation of paleomagnetic data between sections. The circles represent Schmidt stereographic projections for inclinations greater than 50°. A separate projection is provided for each phase of volcanism which shows its unit mean remanence directions. Remanence vectors with normal (+ve) downward and reversed (-ve) upward inclinations are shown as circles and crosses respectively.

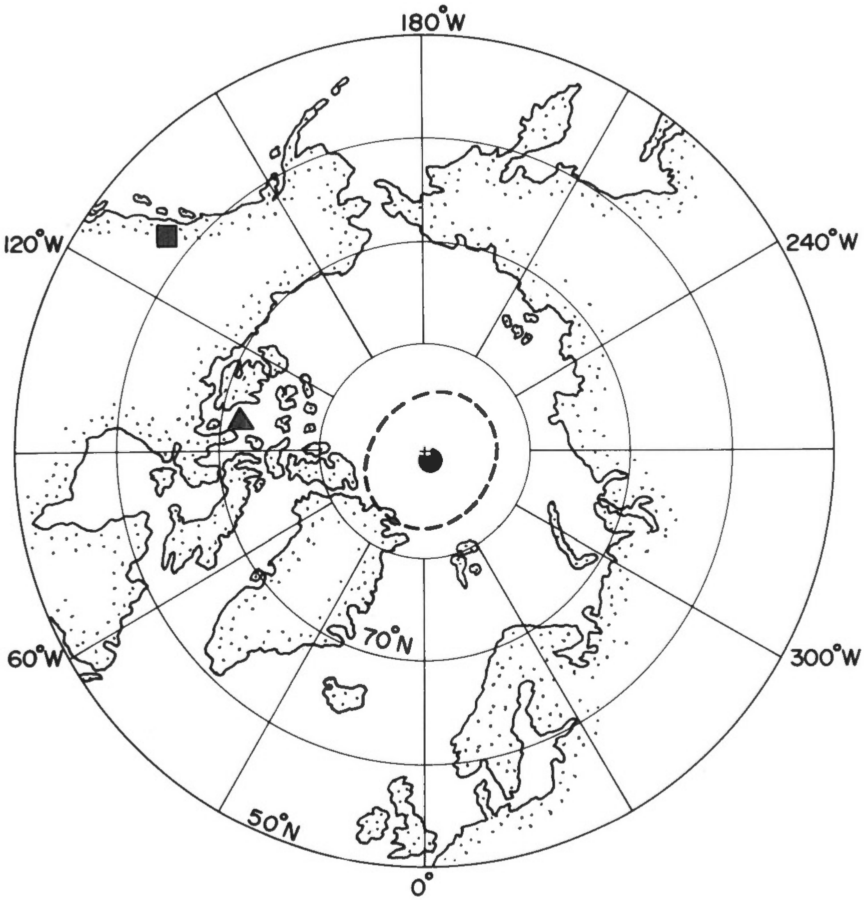


Figure 10. Projection of northern hemisphere above latitude 50° N. The square is the Mount Edziza sampling site. The circle is the pole position for the 84 lava flows as given in Appendix III part 2 along with its oval of 95% confidence. The triangle is the earth's present north magnetic pole.

structure and stratigraphy of Mount Edziza are much more complex than that of a single, symmetrical cone. Mapping done subsequent to the paleomagnetic sampling has shown that the present cone and crater are very young features, superimposed on the eroded remnants of at least three older volcanic piles. The three measured sections, chosen symmetrically with respect to the present central crater thus include volcanic and intravolcanic deposits laid down during at least four major cycles of volcanicity. Moreover, the shifting position of eruptive centres with time and rapid erosion during periods of dormancy have combined to leave a fragmentary record that is only partly preserved in any one section.

The ten phases of activity for which a record is preserved in the measured sections represent only a small fraction of the total number of pulses of activity. Their relationship to a generalized succession for the entire complex is shown in Figure 7.

Correlation with the paleomagnetic time scale is controlled mainly by the radiometric age dates. The 4.9 to 6.1 m.y. ages for phase 1 and 2 basalt and rhyolite and the 4.0 to 4.3 m.y. age of phase 4 basalt place fairly rigid limits on the phase 4 and older rocks. In Figure 8 the normally magnetized flows of subphase $1_1$ are assigned to magnetozone 14 (ca. 5.8 to 6.1 m.y.). If we assume that no younger polarity subzones are missing in the stratigraphic columns then the upper phase 4 basalts must have been erupted during polarity event 9 (ca. 3.9 to 4.1 m.y.). This is in good agreement with the K/Ar ages of 4.0 to 4.3 m.y. on basalt of the phase 4 assemblage.

The 1.16 m.y. age on rhyolite flows that contributed clasts to unit C12 places a maximum age on phase 6 and younger assemblages. Glacial tills and subglacial hyaloclastites in that part of the section suggest a Pleistocene age which is compatible with the paleomagnetic and radiometric age data.

Phase 10 flows clearly belong to the geologic Recent or polarity event 1. The predominantly subglacial products of phase 10, were probably erupted during a major readvance of alpine glaciers, 2,600 to 2,800 years B.P., that followed the post-Wisconsin retreat (Porter and Denton, 1967).

## DISCUSSION

The paleomagnetic polarity profiles and radiometric ages indicate that Mount Edziza has erupted periodically for at least the last six million years. The remanence directions of individual units erupted during any given phase tend to be closely clustered whereas there is considerable divergence of direction and polarity between phases (Fig. 9). This suggests that several flows were produced in rapid succession during sporadic bursts of activity and that relatively long periods of quiescence, during which the magnetic pole shifted or changed polarity, commonly intervened between episodes of activity. Thus the otherwise similar flows of subphases $1_1$, $1_2$, $1_3$, and $1_4$ were clearly erupted in four separate pulses separated by sufficient time for the earth's magnetic field to change polarity. With the exception of phase 2 all subsequent phases show a similar close grouping of unit mean remanence directions. Divergence in the directions of phase 2 rocks is consistent with the diversity of rock types and the presence of thick fluvial horizons, both of which indicate that phase 2 spanned a considerable interval of time.

Throughout its long history Mount Edziza has yielded a remarkably uniform primary magma. Alkali olivine basalt is by far the most abundant and most widely distributed material within the Edziza pile, and through fractional crystallization, it has given rise to the relatively small volume of associated trachyte and rhyolite. The production of primary basalt occurred in four successive stages of diminishing volume. These began about 6 m.y., 5 m.y., 1 m.y., and 0.5 m.y. B.P. Basalt produced during any given stage may display minor textural and mineralogical variations that are helpful for local correlation but of no regional significance. Similarly acid lava erupted during phases 5 and 8 appears to be unique to Mount Edziza, the products of fractionation in local magma chambers rather than progressive change in the character of regional volcanicity. In this respect it is significant that basalt erupted alternately with rhyolite during phase 5 is mineralogically similar to basalt throughout the remainder of the pile.

Mount Edziza is typical of a large number of volcanoes that lie along the eastern margin of the Coast Geanticline. Although the others have not been studied in detail, random specimens from many of them indicate that alkali olivine basalt is the characteristic magma type of the region. It probably reflects a fundamental style of tectonism that has persisted in the northwestern Cordillera throughout Late Tertiary and Quaternary time. The alkaline to peralkaline nature of the Edziza lavas is analogous to rocks of the Afar depression of east Africa, where peralkaline volcanism is related to crustal separation along the rift-in-rift axis of the Red Sea and Gulf of Aden (Barberi et al., 1972). Moreover the distribution of Mount Edziza and neighbouring volcanoes along a north-south zone of block faulting suggests that the lava ascended along tension fractures. These may have formed in response to right lateral movement on northwesterly trending transcurrent faults at the continental margin (Souther, 1970). Such movement is known to have taken place along the Fairweather and related faults (Page, 1969) during approximately the same interval of time that Mount Edziza evolved.

## REFERENCES


Barberi, F., Tazieff, H., and Varet, J.
1972: Volcanism in the afar depressions: its tectonic and magmatic significance; Tectonophysics, v. 15, no. (1/2), p. 17-29.

Cox, A.
1969: Geomagnetic reversals; Science, v. 163, p. 273-245.

Cox, A., and Dalrymple, G. B.
1967: Statistical analysis of geomagnetic reversal data and the precision of potassium-argon dating; J. Geophys. Res., v. 72, p. 2603-2614.

Fisher, R.A.
1953: Dispersion on a sphere; Proc. Royal Soc. Ser. A, v. 217, p. 295.

Heirtzler, J.R., Dickson, G.O., Herron, E.M., Pitman, W.C., III, and Le Pichon, S.
1968: Marine magnetic anomalies, geomagnetic field reversals, and motions of the ocean floor and continents; J. Geophys. Res., v. 73, p. 2119-2136.

Kuno, H.
1968: Differentiation of basalt magmas; in the Poldervaart Treatise on Rocks of Basaltic Composition, Interscience Publishers, v. 2, p. 627.

1969: Andesite in time and space; Proc. of the Andesite Conference, Int. Upper Mantle Project, Scientific Report 16, p. 14.

Lambert, M.B.
1968: Wheaton River and Homan Lake, Yukon and British Columbia (105 D/5, 105 M/14), in Report of Activities, May to October 1967, Geol. Surv. Can., Paper 68-1, Pt. A, p. 32.

Larochelle, A.
1968: L'application de la statistique au paléomagnétisme; Geol. Surv. Can., Paper 68-59, 19 pp.

Larochelle, A., and Black, R. F.
1965: The design and testing of an alternating field demagnetizing apparatus; Can. J. Earth Sci., v. 2, p. 684-696.

Larochelle, A., and Christie, R. F.
1967: An automatic 3-magnet or biastatic magnetometer; Geol. Surv. Can., Paper 67-28, 28 pp.

Lowdon, J. A., Fyles, J. G., and Blake, W. J.
1967: Radiocarbon dates VI; Geol. Surv. Can., Paper 67-2, Pt. B., p. 19.

Mathews, H. W.
1958: Geology of the Mount Garibaldi map-area, southwestern British Columbia, Canada. Part II. Geomorphology and Quaternary volcanic rocks. Bull. Geol. Soc. Amer., v. 80, p. 1873-1877.

Porter, S. C., and Denton, G. H.
1967: Chronology of Neoglaciation in the North American Cordillera, Am. J. Sci., v. 265, March, 1967, p. 177.

Rouse, G. E., and Mathews, W. H.
1961: Radioactive dating of Tertiary plant-bearing deposits; Science, v. 133, p. 1079-1080.

Souther, J. G.
1967: Acid volcanism and its relationship to the tectonic history of the Cordillera of British Columbia; Bull. Volcanologique, v. 30, p. 161-176.

1970: Volcanism and its relationship to recent crustal movements in the Canada Cordillera; Can. J. Earth Sci., v. 7, no. 2, p. 553-568.

1971: Geology and mineral deposits of Tulsequah map-area, British Columbia; Geol. Surv. Can., Mem. 362.

1972: Physical Evolution of Mount Edziza Volcanic Complex; Vol. and Soc. Japan, J., 1972.

Tarling, D. H., and Symons, D. T. A.
1967: A stability index of remanence in paleomagnetism; Roy. Astron. Soc. Geophys. J., v. 12, p. 443-448.

Wilson, R. L.
1971: Dipole offset - the time-average paleomagnetic field over the past 25 million years; Roy. Astron. Soc. Geophys. J., v. 22, p. 491-504.

Yagi, K., and Souther, J. G.
(in prep.) Aenigmatite from Mount Edziza, British Columbia.

# APPENDICES

## Appendix I

Description of Stratigraphic Sections
- Section A
- Section B
- Section C

## Appendix II

Part 1: Petrographic data on lavas from stratigraphic sections A, B, and C.

Part 2: Modes of lavas from central cone on Mount Edziza.

## Appendix III

Part 1: Paleomagnetic remanence data by sites.

Part 2: Mean remanence direction statistics.

# APPENDIX I

## Description of Stratigraphic Sections

Section A

| Unit No. | Thickness (in ?) | Cumulative Thickness (in ?) | |
|---|---|---|---|
| A28 | 15 | 926 | Basalt flow; rough clinkery surface with prominent troughs and lava levees; medium grey, black weathering; vesicular; moderately porphyritic with 2 to 5 mm ragged phenocrysts of clear white feldspar and sparse 1 to 3 mm phenocrysts of olivine and pyroxene. |
| A27 | 14 | 911 | Basalt flow; same as above. |
| A26 | 12 | 897 | Trachybasalt intracanyon flow; medium grey, light grey weathering; large diameter, well-developed columns and prominent horizontal, platy flow cleavage; sparse phenocrysts of tabular feldspar to 1 cm. |
| A25 | 17 | 885 | Colluvium; well-rounded fluvial gravel in a grey earthy matrix. |
| A24 | 20 | 868 | Basalt flow; medium grey, brown weathering; random, irregular jointing, coarsely porphyritic with abundant plagioclase phenocrysts up to 2 cm in diameter and olivine and pyroxene phenocrysts up to 5 mm in diameter. |
| A23 | 18 | 848 | Fluvial layer; well-rounded and sorted boulders and cobbles of locally derived rocks in a sandy, hematite-stained matrix. |
| A22 | 20 | 830 | Trachybasalt flow, light greenish grey, green weathering; small well-developed columns, prominent horizontal platy joints and flow structure; planar alignment of groundmass feldspar and sparse 3 to 4 mm tabular feldspar phenocrysts give the rock a distinctive laminated fabric and lustrous surface resembling phyllite. |

Section A (cont'd)

| Unit No. | Thickness (in ?) | Cumulative Thickness (in ?) | |
|---|---|---|---|
| A21 | 20 | 810 | Colluvium; unsorted, well-rounded fluvial boulders and pebbles mixed with angular rock fragments in an earthy to sandy unconsolidated matrix. |
| A20 | 75 | 790 | Basalt flow, medium grey, rusty weathering; widely spaced irregular polygonal jointing; coarsely porphyritic with clear, tabular feldspar phenocrysts forming 20 to 40 per cent of rock. |
| A19 | 15 | 715 | Basaltic scoria, brick red, unwelded, loosely compacted bombs and lapilli; lower part contains well-rounded, hematite-stained fluvial boulders in a red earthy matrix. |
| A18 | 15 | 690 | Basalt flows; four thin, closely related flows separated by thin layers of loosely welded scoria; except for short columns at the top of each flow the unit is randomly jointed; medium grey, non-porphyritic, highly vesicular. |
| A17 | 5 | 685 | Basaltic scoria; loose, unwelded bombs and lapilli. |
| A16 | 20 | 680 | Basalt flow, light grey, grey weathering; crude, irregular columns; highly vesicular fine grained with sparse tabular feldspar phenocrysts up to 1 cm across. |
| A15 | 5 | 660 | Basaltic scoria, welded spatter, bombs and lapilli, brick red, highly oxidized. |
| A14 | 25 | 655 | Basalt flow, dark bluish grey, rusty weathering well-developed columnar jointing; fine-grained dense rock with 15% feldspar phenocrysts up to 2 cm. |
| A13 | 5 | 630 | Glacial till, unsorted and unstratified boulders and cobbles in a compacted sandy clay matrix; includes rocks that are not indiginous to the volcano. |

Section A (cont'd)

| Unit No. | Thickness (in ?) | Cumulative Thickness (in ?) | |
|---|---|---|---|
| A12 | 15 | 625 | Basaltic scoria and thin discontinuous flow tongues; mainly highly vesicular, oxidized cinders and unwelded clinker; flows are dark grey, highly vesicular, randomly jointed, spheroidal-weathering basalt. |
| A11 | 25 | 610 | Basalt flow; dark bluish grey, reddish brown-weathering; well-developed short thick columns and prominent horizontal fluidal structure and platy flow cleavage; fine grained with sparse 2 to 4 cm phenocrysts of clear plagioclase and rare carbonate amygdules. |
| A10 | 55 | 585 | Basalt flow; medium grey, light grey weathering, well-developed long thin columns, prominent horizontal flow cleavage, fine grained, non-porphyritic. |
| A9 | 10 | 530 | Basaltic scoria; unwelded, limonite stained cinders and clinker. |
| A8 | 25 | 520 | Basalt flow; medium grey, rusty weathering; random, poorly developed jointing, fine grained, non-porphyritic, with a few small cavities partly filled with aragonite and goethite. |
| A7 | 25 | 495 | Basalt flow; light bluish grey, rusty weathering; well-developed thin columns, fine grained with sparse 2 to 5 mm tabular phenocrysts of plagioclase. |
| A6 | 5 | 470 | Basaltic scoria; unwelded, limonite-stained cinders and clinker. |
| A5 | 50 | 465 | Basalt flow; black, rusty weathering; small, well-developed columns; fine grained to glassy, non-porphyritic; upper part of flow contains aragonite filled cavities. |

Section A (cont'd)

| Unit No. | Thickness (in ?) | Cumulative Thickness (in ?) | |
|---|---|---|---|
| A4 | 70 | 415 | Covered; recessive unit |
| A3 | 65 | 345 | Basalt flow; medium grey, rusty weathering; well-developed columns radiate outward from a central massive core; fine grained to glassy, hard, brittle rock with sparse phenocrysts of clear tabular plagioclase to 1 cm. |
| A2 | 45 | 280 | Covered; recessive unit. |
| A1 | 235 | 235 | Basalt flow; medium grey, rusty weathering; well-developed curvi-columnar joints arranged in fans and rosettes; lower part of flow is dense, fine grained, non-porphyritic, upper part is highly vesicular containing voids up to 5 cm across filled with radial clusters of aragonite crystals or lined with botryoidal goethite. |

Base of section: contact with underlying Tertiary conglomerate covered by thin layer of white ash.

Section B

| Unit No. | Thickness (in ?) | Cumulative Thickness (in ?) | |
|---|---|---|---|
| B53 | 60 | 1521 | Basaltic hyaloclastite; well-bedded, yellowish brown palagonite tuff fragments, mainly less than 1 cm but some beds contain angular chunks of vesicular glassy basalt from 5 to 20 cm; loosely welded. |
| B52 | 22 | 1461 | Basaltic hyaloclastite; pillow breccia comprising granular palagonite tuff enclosing wedge-shaped fragments of highly vesicular pillows and a few whole pillows of black glassy basalt with small white feldspar phenocrysts; numerous 2 to 10 cm accidental inclusions of white, partly fused granitic rock. |
| B51 | 12 | 1439 | Basalt flow; light grey, light green weathering; small well-developed columns, prominent horizontal platy joints and flow structure; fine grained with numerous phenocrysts of pyroxene and small tabular feldspars. |
| B50 | 6 | 1427 | Colluvium, well-rounded fluvial gravel in a sandy, hematite-stained matrix. |
| B49 | 20 | 1421 | Basalt flow; light brownish grey, yellowish brown weathering; short thick columns near base; entire flow highly vesicular, pipe vesicles at base, upper part contains irregular cavities up to 10 cm across; fine grained, non-porphyritic. |
| B48 | 11 | 1401 | Basalt flow; same as unit 49. |
| B47 | 14 | 1390 | Basalt flow; same as unit 49. |
| B46 | 3 | 1376 | Basalt flow; same as unit 49. |

Section B (cont'd)

| Unit No. | Thickness (in ?) | Cumulative Thickness (in ?) | |
|---|---|---|---|
| B45 | 20 | 1373 | Glacial till; unsorted hematite-stained cobbles and boulders up to 18 inches in diameter in a grey, silty clay matrix, boulders are mainly Edziza basalt but older volcanic rocks and granitic rocks are also present; upper half of unit contains abundant brick red basaltic ash and fine lapilli. |
| B44 | 3 | 1353 | Basalt flow; bluish grey, brown speroidal weathering; short thick columns; fine grained with sparse, clear feldspar phenocrysts up to 1 cm across. |
| B43 | 5 | 1350 | Basalt flow; medium bluish grey, rusty weathering; short thick columns at base; fine grained with sparse, clear feldspar phenocrysts up to 1 cm across. |
| B42 | 14 | 1345 | Basalt flow; medium bluish grey, lustrous brown weathering; lower three feet slaggy, porous clinker, central part dense columnar jointed lava with few vesicles, upper two feet highly vesicular; fine grained moderately porphyritic with clear tabular feldspar phenocrysts from 1 to 2 cm long. |
| B41 | 14 | 1331 | Basalt flow; medium grey, rusty weathering; crude polygonal jointing; vesicular throughout; fine grained, moderately porphyritic with abundant tabular feldspar phenocrysts up to 2 cm across. |
| B40 | 4 | 1317 | Basaltic scoria; brick red, unwelded bombs and lapilli. |
| B39 | 25 | 1313 | Basalt flow; bluish grey, lustrous brown weathering; well-developed columns with a tendency to spheroidal weathering; fine grained with sparse tabular 2 to 10 mm phenocrysts of clear feldspar and small glomeroporphyritic clusters of feldspar and pyroxene. |

Section B (cont'd)

| Unit No. | Thickness (in ?) | Cumulative Thickness (in ?) | |
|---|---|---|---|
| B38 | 20 | 1288 | Basaltic lapilli ash; brick red, loosely welded, crudely stratified. |
| B37 | 40 | 1268 | Basalt flow; bluish grey, rusty weathering; long, perfectly developed columns; fine grained, slightly porphyritic, with sparse phenocrysts of clear tabular feldspar. |
| B36 | 20 | 1228 | Basalt flow; bluish grey, reddish brown weathering; poorly developed columns at base, random jointing in upper part; fine grained, highly porphyritic with 20 to 50 per cent clear, tabular feldspar phenocrysts from 2 to 4 cm across. |
| B35 | 5 | 1208 | Basalt flow; medium grey, black to rusty weathering; short columns about 10 inches in diameter; highly vesicular throughout with prominent subhorizontal vesicle layers; all joints and cavities deeply stained with Fe-Mn oxides; fine grained, non-porphyritic; base rests on hematite-stained fluvial pebbles of Edziza basalt in a sandy matrix. |
| B34 | 25 | 1203 | Basalt flow; same as unit 35. |
| B33 | 15 | 1178 | Basalt flow; bluish grey, lustrous brown-weathering; short, poorly developed spheroidal-weathered columns; fine grained with sparse very thin tabular phenocrysts of plagioclase from 1 to 3 cm long. |
| B32 | 65 | 1163 | Rhyolitic ash fall; white, unwelded pumiceous ash containing from 10 to 20% 5- to 10-mm tabular plagioclase crystals and a few small euhedral prisms of amphibole. |

Section B (cont'd)

| Unit No. | Thickness (in ?) | Cumulative Thickness (in ?) | |
|---|---|---|---|
| B31 | 12 | 1098 | Basalt flow; blue grey, brown weathering; poorly developed columns at base, random joints in upper part; very fine grained to glassy, non-porphyritic. |
| B30 | 18 | 1086 | Basalt flow; dark grey to black, dark brown weathering; random blocky jointing; very fine grained to glassy, non-porphyritic. |
| B29 | 25 | 1068 | Rhyolitic ash flow; pale grey with lenses of black porphyritic glass from 10 to 50 cm long; light yellow weathering; highly welded pumiceous matrix surrounds numerous crystal and lithic fragments. |
| B28 | 15 | 1043 | Fluvial gravel; hematite-stained pebbles and boulders of Edziza lavas in a red earthy matrix. |
| B27 | 60 | 1028 | Rhyolitic ash flow; upper part pale grey, base black, light yellow to orange weathering; highly welded pumiceous matrix surrounds numerous crystal and lithic fragments. Includes at least two cooling units. |
| B26 | 50 | 968 | Fluvial gravel; well-sorted pebbles and boulders of mixed volcanic rocks in a sandy matrix containing a high proportion of pumiceous ash. |
| B25 | 20 | 918 | Glacial fluvial; lower half unsorted, randomly oriented cobbles and boulders in a sandy clay matrix; upper half, well-sorted and stratified fluvial gravel comprising well-rounded pebbles from 1 to 10 cm in diameter. |
| B24 | 81 | 898 | Pumiceous ash fall; fine, white, unwelded ash containing 10 to 20% clear feldspar crystals and a trace of magnetite. |

Section B (cont'd)

| Unit No. | Thickness (in ? ) | Cumulative Thickness (in ? ) | |
|---|---|---|---|
| B23 | 20 | 817 | Basalt flow; dark grey to black, dark brown weathering, poorly developed columns; very fine grained, hard, brittle, non-porphyritic. |
| B22 | 10 | 797 | Basalt flow; same as unit 23. |
| B21 | 11 | 787 | Basalt flow; same as unit 23. |
| B20 | 15 | 776 | Fluvial gravel; coarse, unsorted gravel at base, grading upward into fine, laminated ashy beds; yellow weathering, poorly indurated. |
| B19 | 33 | 761 | Lahar; randomly oriented, angular and a few rounded clasts of mainly basalt in a brownish yellow ashy matrix; includes blocks up to one metre across, also pockets and streaks of black as well as oxidized basaltic cinders; upper part shows evidence of reworking. |
| B18 | 8 | 728 | Basalt flow; medium grey, dark brown weathering; random jointing, much infolded scoria, numerous elliptical and irregular gas holes up to 30 cm across lined, with botryoidal iron oxides, zeolites, and aragonite; fine grained, non-porphyritic. |
| B17 | 76 | 720 | Fluvial layer; well-rounded and stratified pebbles and cobbles of white, porphyritic rhyolite in a white ashy matrix. |
| B16 | 61 | 644 | Pumiceous ash fall; white, white to light yellow weathering, very fine grained, unwelded ash containing a few small feldspar crystals. |

Section B (cont'd)

| Unit No. | Thickness (in ?) | Cumulative Thickness (in ?) | |
|---|---|---|---|
| B15 | 30 | 583 | Basalt flow; medium grey, reddish brown weathering, large diameter crudely developed columns; medium grained, non-porphyritic. |
| B14 | 32 | 553 | Basalt flow; medium grey with prominent amber coloured phenocrysts, reddish brown weathering; widely spaced irregular jointing; highly porphyritic, containing 30 to 50% clear to pale yellow, tabular feldspar phenocrysts from 5 mm to 3 cm across. |
| B13 | 94 | 521 | Basalt; mainly scoria and lightly welded flow breccia; central part is porphyritic lava similar to unit 14. |
| B12 | | 427 | Basalt flow; lustrous blue grey, brown weathering; short, poorly developed columns; much infolded scoria at base; fine grained, moderately porphyritic, containing 10 to 15% clear feldspar phenocrysts from 3 to 10 mm across. |
| B11 | | | Basalt flow; same as unit 12. |
| B10 | 76 | | Basalt flow; same as unit 12. |
| B9 | | | Basalt flow; same as unit 12. |
| B8 | | | Basalt flow; same as unit 12. |
| B7 | 36 | 351 | Basalt flow; lustrous blue grey, brown weathering; irregular, poorly developed columns; fine grained with less than 1% phenocrysts of clear feldspar. |

Section B (cont'd)

| Unit No. | Thickness (in ?) | Cumulative Thickness (in ?) | |
|---|---|---|---|
| B6 | 10 | 315 | Basalt flow; lustrous blue grey, rusty brown weathering; random, blocky jointing; highly porphyritic, containing 30 to 50% clear to pale yellow feldspar phenocrysts from 1/2 to 3 cm across. |
| B5 | 27 | 305 | Basalt flow; lustrous blue grey, brown weathering; lower part massive lava, upper part comprises thin lava lenses mixed with pockets of scoria; fine grained with sparse phenocrysts of clear feldspar from 2 to 10 mm long. |
| B4 | 55 | 278 | Basalt flow; lustrous blue grey, brown weathering; well-developed columns; fine grained with sparse phenocrysts of clear, tabular feldspar up to 3 cm long oriented in horizontal flow layers. |
| B3 | 106 | 223 | Basalt flow; same as unit 4. |
| B2 | 12 | 117 | Basalt flow; same as unit 4. |
| B1 | 105 | 105 | Basalt flow; lustrous very dark grey, black weathering; long slender, curvicolumnar columns; fine grained with less than 1% clear feldspar phenocrysts up to 5 mm long. |

Base of section: Unit 1 rests directly on folded Upper Jurassic mudstone.

Section C

| Unit No. | Thickness (in ?) | Cumulative Thickness (in ?) | |
|---|---|---|---|
| C32 | 28 | 1101 | Basalt flow; light grey, light grey weathering, widely spaced irregular jointing; fine grained matrix, sparse phenocrysts and small crystal aggregates of plagioclase, olivine and pyroxene, accidental clasts of granitic rocks. |
| C31 | 19 | 1073 | Basaltic scoria; brick red, slightly welded cinders and lapilli. |
| C30 | 141 | 1054 | Basalt flows and tuff-breccia; black, black weathering; very fine grained to glassy with perfectly oriented 2 to 4 mm tabular plagioclase phenocrysts; unit is characterized by highly irregular flow tongues, lava tubes and isolated masses of basalt surrounded by black, glassy tuff-breccia; small, polygonal columns, perfectly developed in the lava are always perpendicular to contacts with the enclosing tuff-breccia and to the smooth glassy inner surfaces of lava tubes; both flows and tuff-breccia contain accidental clasts of partly fused granitic rock. |
| C29 | 18 | 913 | Basalt flow; medium grey, medium grey weathering; crude columnar jointing at base, upper half randomly jointed and highly vesicular; fine grained with sparse 2 to 4 mm tabular plagioclase and rounded pyroxene phenocrysts. |
| C28 | 48 | 895 | Basalt flows and tephra; series of overlapping highly vesicular flow tongues enclosing pockets and lenses of bombs, blocks and lapilli; medium grey, rusty weathering; fine grained with abundant 2 to 4 mm randomly oriented phenocrysts of plagioclase; upper four feet brick red, unconsolidated lapilli. |

Section C (cont'd)

| Unit No. | Thickness (in ?) | Cumulative Thickness (in ?) | |
|---|---|---|---|
| C27 | 37 | 847 | Basalt flow and tephra; dark bluish grey, black weathering, crude columnar jointing in lower half, upper half welded spatter and brick red lapilli tuff; fine grained with sparse 2 to 5 mm tabular plagioclase phenocrysts. |
| C26 | 34 | 810 | Basalt flow; dark grey, black weathering; closely spaced three dimensional polygonal joint system (rock breaks into regular, equidimensional polygons about 10 inches in diameter each surrounded by a thick alteration rind); very fine grained with sparse 2 to 4 mm plagioclase phenocrysts. |
| C25 | 18 | 773 | Basalt flow; blue grey, brown weathering; blocky, irregular jointing, much infolded scoria; fine grained with abundant 2 to 8 mm plagioclase phenocrysts and rare phenocrysts to 2 cm across. |
| C24 | 20 | 758 | Basalt flow; same as 25 but lacking large phenocrysts. |
| C23 | 110 | 738 | Recessive unit; mostly covered; in part unconsolidated basaltic cinders. |
| C22 | 34 | 628 | Basalt flow; medium grey, brown weathering; very dense and hard in lower part, upper part lighter coloured and porous; very fine grained with sparse, very thin tabular phenocrysts of plagioclase to 4 mm and rare aggregates of plagioclase and pyroxene. |
| C21 | 21 | 594 | Basalt flow; light brownish grey, rusty weathering, clinkery, highly vesicular; medium grained with moderately abundant, ragged plagioclase phenocrysts to 1 cm and sparse euhedral prisms of black pyroxene. |

Section C (cont'd)

| Unit No. | Thickness (in ?) | Cumulative Thickness (in ?) | |
|---|---|---|---|
| C20 | 46 | 573 | Trachybasalt flow; light brownish grey with prominent darker grey flow bands; blocky irregular jointing, highly vesicular in upper half; fine grained with abundant 4 to 10 mm plagioclase phenocrysts; contains many infolded pockets of scoria, bombs and coarse tephra. |
| C19 | 25 | 527 | Basaltic scoria; red, oxidized, highly vesicular blocks and clinker. |
| C18 | 24 | 502 | Trachybasalt flow; medium grey, brown spheroidal weathering; random, blocky jointing, fine grained with sparse 1 to 2 cm plagioclase, and 2 to 5 mm phenocrysts of pyroxene; contains crystal aggregates of plagioclase and pyroxene up to 10 cm across. |
| C17 | 51 | 478 | Trachybasalt flow; same as unit 18. |
| C16 | 39 | 427 | Basaltic tephra; brick red, highly oxidized; very coarse cinders enclosing large blocks, bombs and accretionary lava balls. |
| C15 | 38 | 388 | Trachybasalt flow; steel grey, brown weathering; well developed, short, thick columns in lower part; fine grained with oriented 5 to 10 mm tabular plagioclase and 2 to 5 mm euhedral phenocrysts of pyroxene. |
| C14 | 31 | 350 | Basalt flow; same as unit 15. |
| C13 | 61 | 319 | Basalt flow; light brownish grey, yellowish brown weathering; massive; fine grained highly porphyritic with very abundant; amber coloured, 1- to 3-cm plagioclase and sparse black 2- to 5-mm pyroxene phenocrysts. |

Section C (cont'd)

| Unit No. | Thickness (in ?) | Cumulative Thickness (in ?) | |
|---|---|---|---|
| C12 | 57 | 258 | Glacial deposit; lower half of unit is sideromelane tuff-breccia containing random, stream-worn boulders; upper half is glacial till containing unsorted cobbles and boulders in a silty clay matrix, boulders include granitic and sedimentary rocks that are not indigenous to the volcano as well as basalt, rhyolite and obsidian from older members of the Edziza pile; unit passes laterally into stratified channel deposits of glacial-fluvial sand and gravel. |
| C11 | 32 | 201 | Basalt flow; dark grey, black weathering with rusty patches; random, blocky jointing; fine grained moderately porphyritic with abundant 2 to 10 mm clear, tabular, amber coloured plagioclase phenocrysts perfectly oriented in flow layers; upper 10 feet sideromelane tuff-breccia. |
| C10 | 13 | 169 | Basalt flow; steel grey, brown weathering; crude columnar jointing in lower half, upper half slaggy, highly vesicular; fine grained, non-porphyritic. |
| C9 | 25 | 156 | Basalt flow; same as unit 10. |
| C8 | 15 | 131 | Basalt flow; medium grey, brown spheroidal weathering; good columnar jointing; fine grained, slightly porphyritic with sparse 5- to 10-mm phenocrysts of clear tabular plagioclase. |
| C7 | 12 | 116 | Basalt flow; medium grey, brown weathering; random jointing; fine grained with rare phenocrysts of clear amber coloured plagioclase up to 2 cm across; highly vesicular; amygdules of aragonite and iron oxides in upper part. |

Section C (cont'd)

| Unit No. | Thickness (in ?) | Cumulative Thickness (in ?) | |
|---|---|---|---|
| C6 | 18 | 104 | Basalt flow; medium grey, brown weathering; random jointing; very fine grained to aphanitic, non-porphyritic. |
| C5 | 27 | 86 | Basalt flow; steel grey, light grey weathering with rusty stain on joint surfaces; bold cliff-forming member with widely spaced rectangular joint system; medium grained with sparse 5- to 10-mm phenocrysts of clear plagioclase. |
| C4 | 15 | 59 | Basalt flows and scoria; medium grey, brown weathering; series of irregular flow tongues interlayered with pockets and lenses of scoria; aphanitic to glassy, non-porphyritic. |
| C3 | 12 | 44 | Basalt flow; steel grey; weathers grey with rusty stain on joint surfaces; random to crudely columnar jointing; fine grained, slightly porphyritic with 5- to 20-mm phenocrysts of clear plagioclase; scoriaceous top containing aragonite-filled amygdules. |
| C2 | 10 | 32 | Basalt flow; same as unit 3. |
| C1 | 22 | 22 | Basalt flow; steel grey with rusty stain on joint surfaces; short poorly formed columns; fine grained, slightly porphyritic with 2- to 4-mm tabular plagioclase phenocrysts oriented in prominent flow layers. |
| | | | Base of section: Unit 1 rests on an earthy regolith overlying hydrothermally altered Triassic greywacke. |

# APPENDIX II

## Part 1: Petrographic data on lavas from stratigraphic sections A, B, and C

| Phase of Volcanic Activity | Unit No. | Total pheno % | MODE, VOLUME PER CENT ** Total feldspar g.m. | Total feldspar pheno | Clino-pyroxene g.m. | Clino-pyroxene pheno | Olivine g.m. | Olivine pheno. | Opaque min. | Glass | Alteration prod. | Lithic clasts | Plagioclase % An of cores *** g.m. | Plagioclase pheno. | Alk. Feldspar % of total feldspar* | Alk. Feldspar Type | Pyroxene Type | Pyroxene 2V | Minor constituents | Texture |
|---|---|---|---|---|---|---|---|---|---|---|---|---|---|---|---|---|---|---|---|---|
| $10_2$ | A28 | 15.5 | 36.4 | 6.8 | 28.3 | 4.0 | 12.7 | 4.6 | 8.2 | --- | --- | --- | 62 | 68 | 5 | KPc | Aug | | Sp. | Intergranular |
| | A27 | 7.5 | 38.3 | 3.6 | 30.2 | 1.0 | 14.8 | 2.9 | 9.2 | --- | --- | --- | 60 | 68 | 5 | KPc | Aug | | Sp. | Intergranular |
| | A26 | 15.6 | 39.2 | 11.1 | 27.1 | 2.4 | 9.9 | 2.1 | 8.4 | --- | --- | --- | 60 | 65 | 5 | KPc | Aug | 54° | Sp. | Intergranular, trachytic |
| 8 | A24 | 24.2 | 40.3 | 14.3 | 23.3 | 1.7 | 2.7 | 8.2 | 5.4 | 2.1 | 2.0 | --- | 60 | 63 | 2 | KPc | Aug | | | Intergranular |
| 7 | A22 | 2.1 | 68.2 | 2.1 | 15.4 | --- | 1.8 | --- | 10.4 | 2.1 | --- | | 56 | 54 | 15 | KPc | NaAug | 62° | Hbld. | Intergranular, trachytic |
| 6 | A20 | 21.0 | 47.8 | 21.0 | 3.2 | --- | 0.2 | --- | 16.3 | 5.4 | 6.1 | --- | 52 | 62 | 5 | KPc | TiAug | | Id. | Intergranular |
| 5 | A18 | <1 | 47.0 | --- | 23.4 | --- | 9.0 | --- | 13.0 | 4.1 | 3.5 | --- | 63 | | 5 | KPc | TiAug | | | Diktytaxitic |
| | A16 | 23.5 | 43.4 | 10.6 | 22.6 | 6.6 | 2.7 | 6.3 | 6.0 | 0.6 | 1.2 | --- | 64 | 64 | 5 | KPc | TiAug | 56° | | Intergranular |
| | A14 | 6.5 | 50.9 | 5.9 | 21.6 | 0.6 | 5.7 | --- | 9.0 | 4.2 | 1.1 | --- | 64 | 66 | 5 | KPc | TiAug | 55° | | Ophitic |
| 4 | A12 | <1 | 50.0 | --- | 35.9 | --- | 0.9 | --- | 8.4 | 2.3 | 2.5 | --- | 62 | | 5 | KPc | NaAug | | | Intergranular |
| | A11 | <1 | 47.8 | --- | 35.0 | --- | 4.9 | --- | 11.8 | 0.5 | --- | --- | 64 | | 5 | KPc | NaAug | 69° | | Intergranular |
| | A10 | <1 | 48.8 | --- | 38.6 | --- | 0.1 | --- | 9.8 | 1.3 | 1.4 | --- | 66 | | 5 | KPc | NaAug | | | Intergranular |
| | A8 | <1 | 42.4 | --- | 38.4 | --- | 2.3 | --- | 15.4 | --- | 1.5 | --- | 64 | | 5 | KPc | NaAug | | | Intergranular |
| | A7 | <1 | 48.7 | --- | 37.7 | --- | 1.6 | --- | 9.3 | 0.7 | 2.0 | --- | 62 | | 5 | KPc | NaAug | | | Intergranular |
| 3 | A5 | <1 | 49.8 | --- | 27.0 | --- | 6.4 | --- | 9.3 | 5.4 | 2.1 | --- | 61 | | 5 | KPc | TiAug | | | Ophitic |
| | A3 | 11.0 | 46.8 | 9.2 | 21.6 | 0.6 | 5.9 | 1.2 | 11.2 | 0.5 | 3.0 | --- | 61 | 63 | 10 | KPc | TiAug | | | Subophitic |
| | A1 | <1 | 46.5 | --- | 32.9 | --- | 6.2 | --- | 10.4 | 1.0 | 3.0 | --- | 68 | | 5 | KPc | TiAug | 55° | | Ophitic |
| $10_1$ | B53 | 21.7 | --- | 10.1 | --- | 1.3 | --- | 5.9 | 4.4 | 78.3 | --- | ±1 | | 68 | -- | | | | | Vitroclastic |
| | B52 | 27.9 | --- | 12.8 | --- | 2.5 | --- | 7.2 | 5.4 | 72.1 | --- | ±1 | | 66 | -- | | | | | Vitroclastic |
| 8 | B51 | 2.5 | 44.3 | 1.9 | 33.4 | --- | 3.5 | 0.6 | 11.1 | --- | 5.2 | | 64 | 68 | 2 | KPc | | | | Intergranular, trachytic |
| 5 | B49 | <1 | 53.0 | --- | 27.0 | --- | 5.2 | --- | 8.9 | 1.2 | 4.7 | | 62 | | 5 | KPc | TiAug | | | Diktytaxitic |
| | B48 | <1 | 43.5 | --- | 25.4 | --- | 8.0 | --- | 20.7 | 1.0 | 1.4 | | 64 | | 5 | KPc | TiAug | 55° | | Diktytaxitic |
| | B47 | <1 | 47.2 | --- | 26.5 | --- | 8.2 | --- | 10.6 | 3.4 | 4.1 | | 66 | | 5 | KPc | TiAug | | | Diktytaxitic |
| | B46 | <1 | 49.0 | --- | 25.9 | --- | 9.1 | --- | 11.4 | 1.4 | 3.2 | | 68 | | 5 | KPc | TiAug | | | Diktytaxitic |
| 4 | B44 | 2.2 | 39.5 | 2.2 | 29.3 | --- | --- | --- | 17.3 | 8.5 | 3.2 | | 68 | | 5 | KPc | | | | Intergranular, random |
| | B43 | <1.0 | 49.7 | 1.0 | 28.5 | --- | 1.6 | --- | 9.8 | 6.2 | 3.2 | | 64 | 67 | 10 | KPc | Aug | | Aeg. | Intergranular |
| | B42 | 3.2 | 47.6 | 3.2 | 29.1 | --- | 8.1 | --- | 5.6 | 1.2 | 5.2 | | | | 5 | KPc | TiAug | | | Subophitic |
| | B41 | <1 | 57.0 | --- | 26.2 | --- | --- | --- | 8.5 | 5.6 | 2.7 | | 59 | | 10 | KPc | NaAug | 70° | Aeg. | Intergranular |
| | B40 | <1 | 52.4 | --- | 27.8 | --- | --- | --- | 9.2 | 7.1 | 3.5 | | | | 5 | KPc | | | | Intergranular |
| | B39 | <1 | 52.7 | --- | 27.8 | --- | 2.5 | --- | 10.4 | 2.2 | 4.4 | | 58 | | 5 | KPc | NaAug | | | Intergranular |
| | B37 | <1 | 52.6 | --- | 28.0 | --- | 7.1 | --- | 6.9 | 3.5 | 1.9 | | 62 | | 10 | KPc | NaAug | | | Intergranular |
| | B36 | 7.9 | 40.4 | 7.9 | 30.5 | --- | 0.4 | --- | 9.9 | 9.6 | 1.3 | | 64 | 67 | 10 | KPc | NaAug | 68° | | Intergranular |
| 3 | B35 | <1 | 46.5 | --- | 31.2 | --- | --- | --- | 10.6 | 5.4 | 6.3 | | 62 | | 5 | KPc | TiAug | | | Subophitic |
| | B34 | <1 | 43.7 | --- | 29.2 | --- | --- | --- | 12.4 | 4.1 | 10.6 | | 62 | | 5 | KPc | TiAug | | | Subophitic |
| | B33 | <1 | 40.8 | --- | 31.5 | --- | 4.4 | --- | 15.8 | 1.8 | 5.7 | | 60 | | 5 | KPc | NaAug | | | Intergranular, trachytic |
| 2 | B32 | 40.0 | --- | 40.0 | --- | --- | --- | --- | 1.0 | 51.6 | --- | 10.6 | | | 95 | Sd | | | Aeg. Amp. | Vitroclastic |
| | B31 | <1 | 48.6 | --- | 22.9 | --- | 3.3 | --- | 13.0 | 2.4 | 9.8 | | 58 | | 5 | KPc | NaAug | | | Intergranular, trachytic |
| | B30 | <1.9 | 36.4 | 1.4 | 36.1 | 0.4 | 3.9 | 0.1 | 18.2 | 3.6 | --- | | 60 | 63 | 5 | KPc | NaAug | | | Intergranular |
| | B29 | 16.2 | --- | 16.2 | --- | --- | --- | --- | x | 72.8 | 2.2 | 8.8 | | | 95 | Sd | | | Aeg. | Vitroclastic, welded |
| | B27 | 14.5 | --- | 14.5 | --- | --- | --- | --- | x | 76.3 | 1.7 | 7.5 | | | 95 | Sd | | | Aeg. | Vitroclastic, welded |
| | B24 | 2.6 | --- | 2.6 | --- | --- | --- | --- | --- | 90.2 | --- | 7.2 | | | 100 | Sd | | | Aeg. | Vitroclastic |
| | B23 | <1 | 52.2 | --- | 19.2 | --- | 2.4 | --- | 10.4 | 6.6 | 10.4 | | 58 | | 5 | KPc | NaAug | 72° | | Intergranular, trachytic |

| | | | | | | | | | | | | | | | | | | | |
|---|---|---|---|---|---|---|---|---|---|---|---|---|---|---|---|---|---|---|---|
| | B22 | <1 | 51.5 | --- | 13.4 | --- | 2.5 | --- | 9.8 | 13.2 | 11.4 | | 55 | | 5 | KPc | NaAug | | | Intergranular, trachytic |
| | B21 | <1 | 62.1 | --- | 12.2 | --- | --- | --- | 12.7 | 5.1 | 8.0 | | 58 | | 5 | KPc | NaAug | | | Intergranular, trachytic |
| | B18 | <1 | 74.1 | --- | 4.1 | --- | 1.8 | --- | 6.8 | --- | 13.3 | | 52 | | 5 | KPc | NaAug | | | Intergranular, trachytic |
| | B16 | 1.9 | --- | 1.9 | --- | --- | --- | --- | --- | 93.1 | --- | 5.9 | | | 100 | Sd | | | Aeg. | Vistroclastic |
| $1_4$ | B15 | <1 | 47.0 | --- | 19.4 | --- | --- | --- | 20.1 | 6.2 | 7.3 | | 63 | | 5 | KPc | TiAug | | Id. | Subophitic |
| | B14 | 40.7 | 32.0 | 39.5 | 9.8 | 0.1 | 1.6 | 1.1 | 7.3 | 4.6 | 4.0 | | 59 | 59 | 5 | KPc | TiAug | 52° | Sp. | Intergranular |
| | B13 | 8.8 | 48.6 | 8.8 | 17.6 | --- | 5.4 | --- | 13.5 | 2.8 | 3.3 | | 59 | 62 | 10 | KPc | TiAug | | Sp. | Ophitic |
| | B12 | <1 | 63.3 | --- | 13.1 | --- | 4.2 | --- | 12.0 | --- | 7.3 | | 59 | | 5 | KPc | Aug | | | Subophitic |
| | B11 | <1 | 52.9 | --- | 18.3 | --- | 4.2 | --- | 15.4 | --- | 9.1 | | 55 | | 5 | KPc | TiAug | | | Subophitic, trachytic |
| $1_3$ | B10 | 6.5 | 53.4 | 6.5 | 1.7 | --- | 0.1 | --- | 12.7 | 5.5 | 20.1 | | 54 | 54 | 10 | KPc | TiAug | | | Subophitic, trachytic |
| | B9 | 2.2 | 57.4 | 2.2 | 18.2 | --- | 5.0 | --- | 10.2 | --- | 7.4 | | 50 | 54 | 10 | KPc | Aug | | Sp. | Subophitic |
| | B8 | 6.1 | 50.7 | 5.3 | 15.0 | --- | 2.4 | 0.8 | 14.3 | 1.6 | 9.9 | | 50 | 55 | 5 | KPc | TiAug | | | Subophitic, trachytic |
| | B7 | <1 | 49.0 | --- | 17.8 | --- | 2.4 | --- | 16.2 | 5.2 | 9.4 | | 59 | | 2 | KPc | Aug | | | Subophitic |
| $1_2$ | B6 | 11.4 | 52.6 | 11.4 | 1.4 | --- | 0.9 | --- | 11.7 | 1.8 | 20.2 | | 60 | 69 | 2 | KPc | Aug | | | Intersertal |
| | B5 | <1 | 42.4 | --- | 8.4 | --- | 5.4 | --- | 14.2 | 4.8 | 24.8 | | 61 | | --- | | Aug | | | Intersertal |
| | B4 | <1 | 54.6 | --- | --- | --- | 3.6 | --- | 12.8 | --- | 29.0 | | 58 | | --- | | Aug | | | Intersertal |
| | B3 | <1 | 60.2 | --- | 7.6 | --- | 4.1 | --- | 16.8 | 4.4 | 6.9 | | 58 | | --- | | TiAug | | Sp. | Intersertal |
| $1_1$ | B2 | <1 | 50.1 | --- | 8.6 | --- | --- | --- | 8.2 | --- | 32.4 | | 56 | | 2 | KPc | TiAug | | | Subophitic |
| | B1 | <1 | 50.0 | --- | 17.8 | --- | 13.5 | --- | 10.6 | --- | 8.1 | | 60 | | 2 | KPc | TiAug | | | Subophitic |
| $10_1$ | C32 | 3.1 | 51.3 | 1.8 | 15.9 | 0.6 | 11.2 | 0.7 | 18.5 | --- | --- | | 65 | 68 | 2 | KPc | NaAug | | | Intergranular |
| | C30 | 14.6 | 30.8 | 9.6 | 14.8 | 0.7 | 14.4 | 3.3 | 19.8 | 2.3 | 4.3 | | 65 | 68 | --- | | | | | Intergranular |
| | C29 | 15.3 | 43.7 | 13.8 | 13.6 | 1.0 | 0.8 | --- | 14.0 | 3.2 | 9.9 | | | | 5 | KPc | NaAug | | | Intergranular |
| 9 | C28 | 6.5 | 44.7 | 6.2 | 15.7 | 0.2 | 4.2 | --- | 22.5 | 1.5 | 5.0 | | 60 | 60 | 5 | KPc | NaAug | | | Intergranular |
| | C27 | 8.3 | 41.9 | 6.6 | 20.0 | 0.3 | 2.8 | 1.4 | 19.3 | 3.4 | 4.3 | | 56 | 56 | 5 | KPc | NaAug | 70° | | Intergranular |
| | C26 | 4.3 | 37.3 | 4.3 | 31.9 | --- | 1.3 | --- | 15.8 | 1.4 | 8.0 | | 62 | 66 | 5 | KPc | NaAug | | | Intergranular |
| 8 | C25 | | 20.5 | 34.8 | 10.2 | 5.5 | --- | 7.8 | 21.2 | --- | --- | | | | 2 | KPc | | | | |
| | C24 | 52.2 | 19.1 | 34.2 | 9.6 | 5.5 | --- | 12.0 | 19.6 | --- | --- | | 61 | 69 | 2 | KPc | Aug | | | Intergranular |
| | C22 | 5.8 | 64.0 | 3.8 | 12.9 | 1.9 | 2.6 | 0.3 | 11.9 | --- | 2.8 | | 60 | 64 | 5 | KPc | TiAug | | | Intergranular |
| | C21 | 9.4 | 64.2 | 8.5 | 11.1 | 0.9 | 0.2 | --- | 14.2 | --- | 0.9 | | 56 | 54 | 10 | KPc | NaAug | 72° | Aeg. | Intergranular |
| | C20 | 16.7 | 58.9 | 16.3 | 15.9 | 0.4 | --- | --- | 7.6 | --- | 0.9 | | 59 | 59 | 10 | KPc | NaAug | | Aeg. | Intergranular |
| 7 | C18 | 9.8 | 64.3 | 6.2 | 8.1 | 2.0 | 1.0 | 1.6 | 9.8 | 2.1 | 4.8 | | 50 | 52 | 10 | KPc | NaAug | | Hbld. | Intergranular |
| | C17 | 8.4 | 63.4 | 7.3 | 7.9 | 1.8 | 0.4 | 0.3 | 10.3 | 2.6 | 6.0 | | 52 | 54 | 10 | KPc | NaAug | | Hbld. | Intergranular |
| | C16 | 8.1 | 56.7 | 5.1 | 6.9 | 1.9 | 0.6 | 1.1 | 15.7 | 2.5 | 9.5 | | 54 | 54 | 10 | KPc | NaAug | | Hbld. | Intergranular |
| | C15 | 17.9 | 49.3 | 16.3 | 6.5 | 0.4 | 0.5 | 1.2 | 18.8 | 2.5 | 4.5 | | 60 | 64 | 5 | KPc | Aug | | | Intergranular |
| | C14 | 16.9 | 49.9 | 13.3 | 0.6 | 2.4 | --- | 1.2 | 16.6 | 2.5 | 13.5 | | 60 | 64 | 5 | KPc | TiAug | | Ap | Intergranular |
| | C13 | 35.5 | 33.5 | 33.5 | --- | 1.0 | 0.9 | 1.0 | 16.4 | 1.2 | 12.5 | | 60 | 64 | 5 | KPc | TiAug | | Ap | Intergranular |
| | C11 | 8.9 | 47.6 | 8.5 | 21.7 | --- | 6.0 | 0.4 | 10.2 | 2.2 | 2.4 | | 60 | 68 | 5 | KPc | TiAug | | | Ophitic |
| | C10 | <1 | 36.2 | --- | 23.1 | --- | 3.9 | --- | 23.5 | --- | 13.3 | | 58 | | 5 | KPc | TiAug | | | Ophitic |
| | C9 | <1 | 46.3 | --- | 29.5 | --- | 5.7 | --- | 16.8 | --- | 1.7 | | 60 | | | | TiAug | | | Ophitic |
| | C8 | <1 | 41.0 | --- | 19.3 | --- | 1.8 | --- | 18.3 | --- | 19.6 | | 63 | | | | TiAug | | | Ophitic |
| | C7 | <1 | 56.1 | --- | 20.3 | --- | 5.0 | --- | 13.5 | 1.2 | 3.9 | | 65 | | | | TiAug | | | Ophitic |
| | C6 | <1 | 57.6 | --- | 17.6 | --- | 3.7 | --- | 11.8 | 2.1 | 7.3 | | 58 | | | | TiAug | | | Ophitic |
| 5 | C5 | 5.3 | 51.3 | 5.3 | 22.6 | --- | 6.7 | --- | 10.1 | 1.5 | 2.5 | | 60 | 64 | | | TiAug | | | Ophitic |
| | C4 | <1 | 46.2 | --- | 28.7 | --- | 6.4 | --- | 15.5 | --- | 3.2 | | 58 | | | | TiAug | | | Ophitic |
| | C3 | 1.0 | 51.6 | 1.0 | 26.0 | --- | 8.0 | --- | 13.4 | --- | --- | | 55 | 55 | | | TiAug | 55° | | Ophitic |
| | C2 | 2.0 | 46.6 | 2.0 | 30.0 | --- | 6.0 | --- | 14.8 | --- | 0.6 | | 58 | 60 | | | TiAug | | | Subophitic |
| | C1 | <1 | 48.0 | --- | 31.1 | --- | 10.1 | --- | 8.2 | --- | 2.6 | | 64 | | | | TiAug | | | Ophitic |

* Estimated from sawn surfaces stained with sodium cobaltinitrite

** Based on 1,000 points for non-porphyritic rocks and 3,000 points for porphyritic rocks

*** Estimated from extinction angles of combined Carlsbad-albite twins normal to (010) or maximum extinction angle of albite twins normal to (010)

Abbreviations:

| | | |
|---|---|---|
| Aeg. - Aegirine | Hbld. - Hornblende | pheno. - phenocrysts |
| Amp. - Amphibole | Id. - Iddingsite | Sd. - Sanidine |
| Aug. - Augite (clear) | KPc - Potash plagioclase | Sp. - Spinel |
| g.m. - groundmass | NaAug - Sodic augite (green) | TiAug. - Titanaugite |

## APPENDIX II

Part 2: Modes of lavas from the central cone of Mount Edziza

| Sample No. | $T_1$ | $T_2$ | $R_1$ | | $R_2$ | | $R_3$ | |
|---|---|---|---|---|---|---|---|---|
| **Phenocrysts** | | | | | | | | |
| Plagioclase | 10.0 | --- | --- | | 5.7 | | --- | |
| Anorthoclase | --- | 6.6 | --- | | 17.2 | | --- | |
| Sanidine | 4.8 | 3.4 | 4.0 | | 2.0 | | 22.0 | |
| Aegirine | 1.2 | 1.8 | 2.2 | | Trace | | 1.8 | |
| Aenigmatite | --- | --- | --- | | Trace | | Trace | |
| **Groundmass** | | | | | | | | |
| Alkalic plagioclase | 55.2 | 54.5 | x | | x | | x | |
| Aegirine | 12.1 | 20.2 | x | | x | | x | |
| Arfvedsonite | --- | 5.2 | --- | 93.8 | --- | 75.1 | x | 76.2 |
| Iron ores | 4.7 | 3.9 | 5.1 | | x | | 4.8 | |
| Tridymite | --- | --- | x | | --- | | x | |
| Glass | 9.6 | --- | x | | --- | | 19.6 | |
| Aenigmatite | 2.4 | 4.4 | --- | | --- | | --- | |

( --- absent, x present, amount not determined)

$T_1, T_2$ Stage III trachyte from lava dome on northwest slope of central cone.

$R_1$ Stage I rhyolite from lava flow on northwest slope of central cone.

$R_2$ Stage I porphyritic rhyolite from lava dome on northeast slope of central cone.

$R_3$ Stage I porphyritic rhyolite from a thick lava flow on southeast slope of central cone.

# APPENDIX III

Part 1: Paleomagnetic remanence data by sites

| Flow Unit | Number of Cores* Used | Number of Cores* Rejected | Stability Index | Intensity AF Cleaning oersteds | Mean Remanence Direction: Declination degrees | Inclination + down degrees | Vector Length R | Precision Parameter k | Radius of 95% Confidence α degrees |
|---|---|---|---|---|---|---|---|---|---|
| A-1 | 4 | | 9.5 | 200 | 201.3 | -61.2 | 3.967 | 92 | 7.3 |
| A-1 | 3 | 1D | 16.6 | 200 | 191.2 | -70.2 | 2.991 | 220 | 5.3 |
| A-3 | 2 | 2D | 10.0 | 200 | 178.0 | -63.7 | 1.996 | 245 | 6.3 |
| A-5 | 2 | 2C | 43.4 | 200 | 181.2 | -75.3 | 1.999 | 1137 | 2.9 |
| A-7 | 4 | | 8.5 | 200 | 348.6 | 76.8 | 3.975 | 120 | 6.4 |
| A-8 | 3 | 1G | 26.5 | 200 | 0.1 | 76.3 | 2.980 | 101 | 8.1 |
| A-10 | 4 | | 32.3 | 200 | 5.7 | 64.8 | 3.986 | 210 | 4.8 |
| A-11 | 3 | 1D | 30.8 | 200 | 356.5 | 57.3 | 2.985 | 135 | 7.0 |
| A-12 | 4 | | 25.3 | 200 | 275.6 | 73.5 | 3.982 | 166 | 5.5 |
| A-14 | 4 | | 30.5 | 200 | 247.3 | -69.8 | 3.949 | 59 | 9.2 |
| A-16 | 3 | 1D | 46.4 | 200 | 215.7 | -75.7 | 2.995 | 436 | 3.9 |
| A-18 | 6 | | 86.8 | 200 | 207.4 | -70.2 | 5.987 | 396 | 2.9 |
| A-20 | 3 | 2D | 7.9 | 200 | 12.8 | 71.8 | 2.980 | 99 | 8.2 |
| A-20 | 4 | | 30.5 | 200 | 13.8 | 79.3 | 3.813 | 15 | 17.5 |
| A-22 | 3 | 1D, 1C | 38.6 | 200 | 171.8 | -69.2 | 2.983 | 119 | 7.4 |
| A-24 | 38 | 2C, 2D | 48.6 | 200 | 206.6 | -83.5 | 37.815 | 200 | 1.6 |
| A-26 | 4 | 1D | 29.7 | 200 | 15.1 | 61.0 | 3.997 | 1076 | 2.1 |
| A-27 | 4 | 1G | 17.8 | 200 | 45.6 | 70.7 | 3.866 | 22 | 14.9 |
| A-28 | 5 | | 20.4 | 200 | 312.6 | 77.0 | 4.935 | 62 | 8.0 |
| | | | | | | | | | |
| B-1 | 4 | | 39.1 | 200 | 34.2 | 72.4 | 3.989 | 280 | 4.2 |
| B-2 | 4 | | 114.2 | 200 | 26.4 | 76.2 | 3.988 | 260 | 4.3 |
| B-3 | | 4C | 1.2 | 200 | | | | | |
| B-4 | 4 | | 21.5 | 200 | 88.3 | -67.3 | 3.990 | 290 | 4.1 |
| B-5 | 4 | | 10.4 | 200 | 87.4 | -57.5 | 3.796 | 15 | 18.3 |
| B-6 | 4 | | 27.3 | 200 | 133.0 | -71.3 | 3.757 | 12 | 20.0 |
| B-7 | 3 | 1D | 9.9 | 200 | 191.6 | -59.2 | 2.992 | 263 | 5.0 |
| B-8 | 3 | 1D | 15.5 | 200 | 285.9 | 60.4 | 2.983 | 120 | 7.4 |
| B-9 | 3 | 1G | 2.8 | 200 | 298.1 | 64.6 | 2.958 | 47 | 11.8 |

Part 1: Continued

| Flow Unit | Number of Cores Used | Number of Cores Rejected* | Stability Index | Intensity AF Cleaning oersteds | Mean Remanence Direction: Declination degrees | Inclination + down degrees | Vector Length R | Precision Parameter k | Radius of 95% Confidence α degrees |
|---|---|---|---|---|---|---|---|---|---|
| B-10 | 4 | | 13.3 | 200 | 299.3 | 58.8 | 3.959 | 73 | 8.2 |
| B-11 | 3 | 1D | 8.2 | 200 | 291.5 | 60.6 | 2.992 | 250 | 5.1 |
| B-12 | 2 | 2C | 14.6 | 200 | 295.0 | 58.1 | 1.997 | 356 | 5.3 |
| B-13 | 3 | 1D | 24.0 | 200 | 201.4 | -50.6 | 2.997 | 587 | 3.3 |
| B-14 | 3 | 1G | 32.2 | 200 | 216.4 | -67.4 | 2.926 | 27 | 15.6 |
| B-15 | 3 | 1C | 14.7 | 200 | 186.2 | -51.0 | 2.990 | 193 | 5.8 |
| B-18 | 2 | 1C | 2.8 | 200 | 265.8 | 68.4 | 1.984 | 64 | 12.4 |
| B-21 | 2 | 1G | 22.9 | 200 | 174.4 | -38.6 | 1.997 | 332 | 5.4 |
| B-22 | 2 | 1C, 1G | 1.6 | 200 | 175.1 | -33.0 | 1.996 | 234 | 6.5 |
| B-23 | 2 | 1C, 1G | 25.9 | 200 | 173.8 | 1.0 | 1.970 | 34 | 17.1 |
| B-27 | 17 | 1D | *37.1 | 200 | 149.1 | -74.2 | 16.971 | 550 | 1.5 |
| B-29 | 4 | | 51.0 | 200 | 203.6 | -65.3 | 3.968 | 95 | 7.2 |
| B-30 | 3 | 1C | 4.8 | 300 | 165.2 | -63.8 | 2.995 | 397 | 4.1 |
| B-31 | 4 | | 8.0 | 300 | 164.8 | -56.2 | 3.984 | 195 | 5.0 |
| B-31 | 2 | 2C | 9.3 | 300 | 157.1 | -58.7 | 1.998 | 551 | 4.2 |
| B-33 | 4 | | 59.6 | 300 | 189.7 | -74.4 | 3.984 | 189 | 5.1 |
| B-34 | 3 | | 48.9 | 300 | 173.6 | -72.6 | 2.998 | 1088 | 2.5 |
| B-35 | 2 | 1G | 22.2 | 300 | 175.0 | 88.0 | 1.951 | 21 | 21.9 |
| B-36 | 2 | 1C, 1G | 6.6 | 300 | 226.6 | -34.5 | 1.917 | 12 | 28.6 |
| B-37 | 3 | 1G | 2.6 | 300 | 224.6 | -25.5 | 2.993 | 271 | 4.9 |
| B-39 | 4 | | 23.7 | 200 | 307.3 | 71.8 | 3.988 | 251 | 4.4 |
| B-41 | 3 | 1G | 73.7 | 200 | 301.5 | 75.6 | 2.999 | 2169 | 1.7 |
| B-42 | 4 | | 10.0 | 200 | 298.6 | 76.6 | 3.994 | 465 | 3.3 |
| B-43 | 4 | | 42.0 | 200 | 294.5 | 74.2 | 3.996 | 724 | 2.6 |
| B-44 | 3 | 1G | 80.5 | 200 | 300.7 | 75.7 | 2.997 | 661 | 3.2 |
| B-46 | 4 | | 32.6 | 200 | 194.0 | -59.4 | 3.993 | 424 | 3.4 |
| B-47 | 3 | | 16.4 | 200 | 200.9 | -58.5 | 2.977 | 87 | 8.7 |
| B-48 | 4 | | 44.6 | 200 | 170.3 | -73.3 | 3.441 | 5 | 35.0 |
| B-49 | 4 | | 46.4 | 200 | 178.9 | -52.4 | 3.951 | 61 | 9.0 |
| B-51 | 4 | | 50.6 | 200 | 198.4 | -58.4 | 3.965 | 87 | 7.5 |
| B-52 | | 4C | 8.5 | 300 | | | | | |
| B-53 | | 4C | 7.2 | 300 | | | | | |

Part 1: Continued

| Flow Unit | Number of Cores* Used | Number of Cores* Rejected | Stability Index | Intensity AF Cleaning oersteds | Mean Remanence Direction: Declination degrees | Inclination + down degrees | Vector Length R | Precision Parameter k | Radius of 95% Confidence α degrees |
|---|---|---|---|---|---|---|---|---|---|
| C-1 | 5 | | 14.2 | 200 | 198.6 | -73.4 | 4.969 | 130 | 5.5 |
| C-2 | 4 | | 19.2 | 200 | 203.1 | -72.7 | 3.948 | 58 | 9.2 |
| C-3 | 3 | 1D | 23.5 | 200 | 193.4 | -69.0 | 2.994 | 311 | 4.6 |
| C-4 | 4 | 1D | 13.2 | 200 | 218.7 | -67.9 | 3.991 | 332 | 3.9 |
| C-5 | 4 | | 10.5 | 200 | 193.0 | -67.3 | 3.990 | 293 | 4.1 |
| C-6 | 4 | | 15.3 | 200 | 187.3 | -67.2 | 3.991 | 332 | 3.8 |
| C-7 | 4 | | 29.6 | 200 | 195.3 | -71.2 | 3.987 | 228 | 4.6 |
| C-8 | 4 | | 111.0 | 200 | 191.9 | -72.3 | 3.985 | 203 | 4.9 |
| C-9 | 4 | | 17.9 | 200 | 168.5 | -65.5 | 3.974 | 117 | 6.5 |
| C-10 | 4 | | 23.6 | 200 | 219.4 | -72.8 | 3.957 | 69 | 8.4 |
| C-11 | 3 | 1G | 30.5 | 200 | 208.6 | -74.5 | 2.983 | 116 | 7.5 |
| C-13 | 5 | | 74.3 | 200 | 205.4 | -63.1 | 4.991 | 426 | 3.0 |
| C-14 | 3 | 1G | 15.0 | 200 | 160.9 | -58.7 | 2.951 | 41 | 12.7 |
| C-15 | 4 | | 121.8 | 200 | 157.3 | -82.5 | 3.9 | 91 | 7.3 |
| C-17 | 3 | 1G | 43.1 | 200 | 237.8 | -71.8 | 2.980 | 98 | 8.2 |
| C-18 | 5 | | 31.1 | 200 | 105.1 | -85.2 | 4.975 | 162 | 4.9 |
| C-20 | 6 | | 54.0 | 200 | 220.1 | -69.9 | 5.990 | 510 | 2.5 |
| C-21 | 4 | | 56.4 | 200 | 218.6 | -73.5 | 3.997 | 882 | 2.4 |
| C-22 | 4 | | 103.2 | 200 | 217.5 | -71.9 | 3.987 | 229 | 4.6 |
| C-24 | 4 | 1G | 20.8 | 200 | 250.6 | -71.2 | 3.996 | 789 | 2.5 |
| C-25 | 4 | | 37.9 | 200 | 236.2 | -66.8 | 3.991 | 346 | 3.8 |
| C-26 | 3 | 1D | 7.9 | 200 | 177.7 | -54.6 | 2.987 | 152 | 6.6 |
| C-27 | 4 | | 60.0 | 200 | 159.7 | -66.7 | 3.997 | 935 | 2.3 |
| C-28 | 3 | 1G | 9.9 | 200 | 160.5 | -66.9 | 2.989 | 182 | 6.0 |
| C-29 | 4 | | 21.5 | 300 | 146.1 | -69.8 | 3.970 | 99 | 7.0 |
| C-30 | 2 | 1C, 1G | 38.7 | 200 | 7.6 | 64.1 | 1.999 | 1565 | 2.5 |
| C-32 | 3 | 1D | 17.3 | 200 | 29.3 | 69.5 | 2.990 | 205 | 5.7 |

* The letter corresponds to the list of rejection criteria given in the text.

## APPENDIX III

Part 2: Mean remanence direction statistics.

| Group | Number of Flows | Length of Vector Resultant | Mean Remanence Direction: Declination degrees | Mean Remanence Direction: Inclination + down degrees | Mean Remanence Direction: Precision Parameter k | Mean Remanence Direction: Radius of Cone of 95% Confidence α degrees | Pole Position (degrees): Longitude West | Pole Position (degrees): Latitude North | Pole Position (degrees): Axes of Oval of 95% Confidence $\delta_m$ | Pole Position (degrees): Axes of Oval of 95% Confidence $\delta_p$ |
|---|---|---|---|---|---|---|---|---|---|---|
| Normal flows | 27 | 24.882 | 325.8 | 77.1 | 12.3 | 8.3 | 181.0 | 72.3 | 15.4 | 14.4 |
| Reversed flows | 57 | 54.554 | 189.5 | -68.3 | 22.9 | 4.0 | 356.3 | 81.7 | 6.8 | 5.7 |
| All flows* | 84 | 78.842 | 0.5 | 71.9 | 16.1 | 4.0 | 328.2 | 89.1 | 7.0 | 6.2 |

Note: *Reversed flows reversed to antiparallel position.